Report No. DOT/FAA/NR-91/1

AD-A239 852

AUG 2 6 1991

C

(2)

Project Report
ATC-178

The 1990 Airport Surveillance Radar Wind Shear Processor (ASR-WSP) Operational Test at Orlando International Airport

T.A. Noyes
S.W. Troxel
M.E. Weber
O.J. Newell
J.A. Cullen

17 July 1991

Lincoln Laboratory
MASSACHUSETTS INSTITUTE OF TECHNOLOGY
LEXINGTON, MASSACHUSETTS

Prepared for the Federal Aviation Administration.
Document is available to the public through the National Technical Information Service, Springfield, Virginia 22161.

91 8 23 030

91-08800

TECHNICAL REPORT STANDARD TITLE PAGE

1. Report No.	2. Government Accession No.	3. Recipient's Catalog No.
ATC-178	DOT/FAA/NR-91/1	

4. Title and Subtitle The 1990 Airport Surveillance Radar Wind Shear Processor (ASR-WSP) Operational Test at Orlando International Airport	5. Report Date 17 July 1991
	6. Performing Organization Code
7. Author(s) T.A. Noyes, S.W. Troxel, M.E. Weber, O.J. Newell, J.A. Cullen	8. Performing Organization Report No. ATC-178
9. Performing Organization Name and Address Lincoln Laboratory, MIT P.O. Box 73 Lexington, MA 02173-9108	10. Work Unit No. (TRAIS)
	11. Contract or Grant No. DTFA-01-L-83-4-10579
12. Sponsoring Agency Name and Address Department of Transportation Federal Aviation Administration Systems Research and Development Service Washington, DC 20591	13. Type of Report and Period Covered Project Report
	14. Sponsoring Agency Code

15. Supplementary Notes

This report is based on studies performed at Lincoln Laboratory, a center for research operated by Massachusetts Institute of Technology under Air Force Contract F19628-90-C-0002.

16. Abstract

Lincoln Laboratory, under sponsorship from the Federal Aviation Administration (FAA), is conducting a program to evaluate the capability of the newest Airport Surveillance Radars (ASR-9) to detect hazardous weather phenomena — in particular, low-altitude wind shear created by thunderstorm-generated microbursts and gust fronts. The ASR-9 could provide coverage at airports not slated for a dedicated Terminal Doppler Weather Radar (TDWR) and could augment the TDWR at high-priority (high traffic volume, severe weather) facilities by providing a more rapid update of wind shear products, a better viewing angle for some runways, and redundancy in the event of a TDWR failure.

An operational evaluation of a testbed ASR Wind Shear Processor (ASR-WSP) was conducted at the Orlando International Airport in Orlando, FL during August and September 1990. The ASR-WSP operational system issued five distinct products to Air Traffic Control: microburst detections, gust front detections, gust front movement predictions, precipitation reflectivity and storm motion. This document describes the operational system, the operational products, and the algorithms employed. An assessment of system performance is provided as one step in evaluating the operational utility of the ASR-WSP.

17. Key Words		18. Distribution Statement
Orlando ASR-9 wind shear	operational demonstration evaluation	Document is available to the public through the National Technical Information Service, Springfield, VA 22161.

19. Security Classif. (of this report)	20. Security Classif. (of this page)	21. No. of Pages	22. Price
Unclassified	Unclassified	63	

FORM DOT F 1700.7 (8-72) Reproduction of completed page authorized

ABSTRACT

Lincoln Laboratory, under sponsorship from the Federal Aviation Administration (FAA), is conducting a program to evaluate the capability of the newest Airport Surveillance Radars (ASR-9) to detect hazardous weather phenomena -- in particular, low-altitude wind shear created by thunderstorm-generated microbursts and gust fronts. The ASR-9 could provide coverage at airports not slated for a dedicated Terminal Doppler Weather Radar (TDWR) and could augment the TDWR at high-priority (high traffic volume, severe weather) facilities by providing a more rapid update of wind shear products, a better viewing angle for some runways, and redundancy in the event of a TDWR failure.

An operational evaluation of a testbed ASR Wind Shear Processor (ASR-WSP) was conducted at the Orlando International Airport in Orlando, FL during August and September 1990. The ASR-WSP operational system issued five distinct products to Air Traffic Control: microburst detections, gust front detections, gust front movement predictions, precipitation reflectivity and storm motion. This document describes the operational system, the operational products, and the algorithms employed. An assessment of system performance is provided as one step in evaluating the operational utility of the ASR-WSP.

A-1

TABLE OF CONTENTS

LIST OF ILLUSTRATIONS

LIST OF TABLES

1. EXECUTIVE SUMMARY

Lincoln Laboratory, under sponsorship from the Federal Aviation Administration (FAA), performed an operational test of an experimental Airport Surveillance Radar Wind Shear Processor (ASR-WSP) at the Orlando International Airport (MCO) during the period from August 29 through September 30, 1990. This report provides a description of the radar system, signal processing algorithms and meteorological algorithms used during the ASR-WSP demonstration and an assessment of the system's performance.

The ASR-WSP test followed operational evaluation of the Terminal Doppler Weather Radar (TDWR) testbed, also operated by Lincoln Laboratory. [1] ASR-WSP products were provided to Air Traffic Control (ATC) controllers and supervisors in the Orlando Tower and Terminal Radar Approach Control facility (TRACON) in the simple, operationally-oriented format used for the earlier TDWR demonstration. Five distinct products were provided:

1. Microburst detection
2. Gust front detection
3. Gust front movement prediction
4. Precipitation reflectivity
5. Storm motion

The 1990 test was the first evaluation of ASR-derived wind shear products in an operational setting. The test had two basic objectives:

1. To provide quantitative assessment of the performance of the signal processing and wind shear detection algorithms in the moist, convectively unstable environment of the Florida peninsula; and
2. To obtain feedback from users (air traffic controllers and supervisors).

The first objective was achieved by recording wind shear products generated by the ASR-WSP during the operational test, and then correlating them with observations from the other meteorological sensing systems described in Section 1.3. User feedback was obtained by Lincoln Laboratory observers stationed in the Tower cab and TRACON during the test period and by means of questionnaires distributed to controllers and supervisors at the conclusion of the test period.

1.1. BACKGROUND AND OPERATIONAL APPLICATION

Airport Surveillance Radars (ASR) are coherent pulsed-Doppler radars whose primary function is to detect and track aircraft targets within a 60 nmi radius. The rapid scanning rate (12.5 RPM) and the large elevation beamwidth (4.8-degree half-power beamwidth)

distinguish it from meteorological radars, which scan slowly and have narrow pencil beams. The newest such radar (ASR-9) is being deployed at over 100 airports in the United States.

From 1986 to the present, the FAA ASR-9 program office has sponsored Lincoln Laboratory to evaluate the capability of the ASR-9 to detect low-altitude wind shear (LAWS) [2] phenomena such as microbursts and gust fronts. This capability may be achieved by means of a relatively low-cost modification to existing ASRs which would allow them to detect LAWS without interfering with their primary function of aircraft detection and tracking. [2,3]

The ASR might be used as a LAWS sensor in two applications: 1) as a stand-alone system at airports without a TDWR or Enhanced Low Level Wind Shear Alert System (ELLWAS), or 2) in an integrated mode with either or both of the TDWR and the ELLWAS.

Algorithms for measuring the low altitude wind field and for automatically detecting microbursts and gust fronts were developed using a testbed ASR-WSP operated in Huntsville, AL (1987 and 1988), Kansas City, MO (1989), and most recently Orlando, FL (1990).

1.2. THE ASR-WSP TESTBED

1.2.1. Processing Equipment

The ASR-WSP testbed used during the Orlando evaluation was an ASR-8 modified to emulate the essential features of an ASR-9. The testbed provides nearly identical antenna patterns, scanning rate, transmitted waveform and receiver stability as a production ASR-9. A modular signal processing channel measured weather reflectivity and low-altitude radial wind using data received on both active and passive signal channels. The testbed was physically located on the Orlando airport between the southern end of runways 18L and 17 (see "ASR" in Figure 1).

Figure 2 is a high-level block diagram of the testbed processing and recording system that was attached to the ASR-8. Signals received on the radar's low (active) and high (passive) receiving beams were shunted to Lincoln Laboratory-built receivers, digitized and distributed simultaneously to the real-time data processor and to the high-density data recording system. Both channels employed an inverse range-squared sensitivity time control (STC), cutting off at 12 km (6.5 nmi). Short-range system sensitivity for a filled beam weather target was 0 dBZ with this STC setting.

Signal processing operations -- ground clutter filtering, reflectivity measurement, radial velocity estimation, and data editing (i.e., tests for low signal-to-noise ratio (SNR) and low signal-to-clutter ratio (SCR)) -- were performed using array processing cards interconnected via a VME-bus backplane. A single-board computer in the same backplane managed the data I/O and performed control operations. Section 2 describes in more detail this processor, the signal processing algorithms employed during the 1990 operational test, and planned upgrades for subsequent tests.

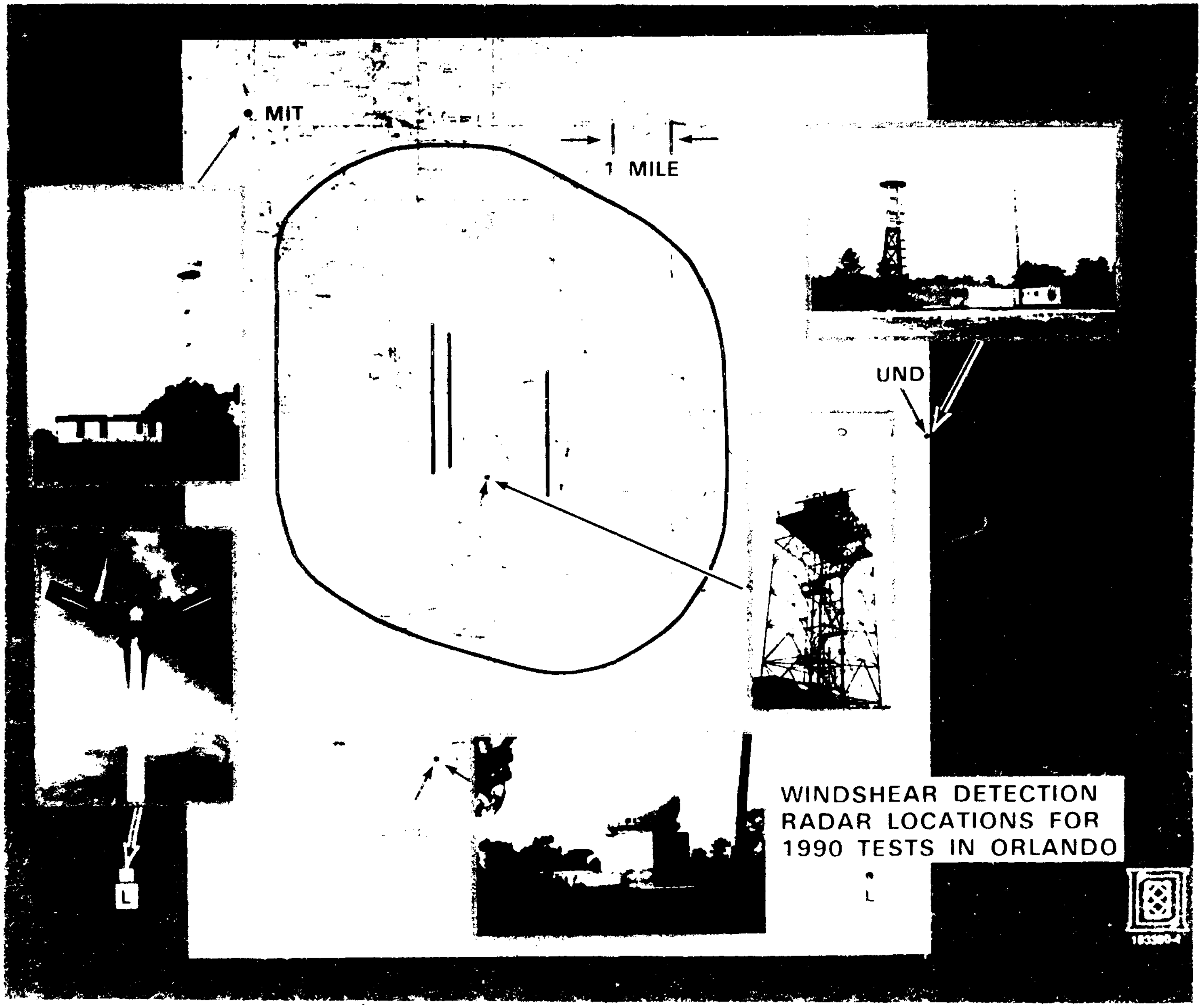

Figure 1. Test Facilities at the Orlando International Airport.

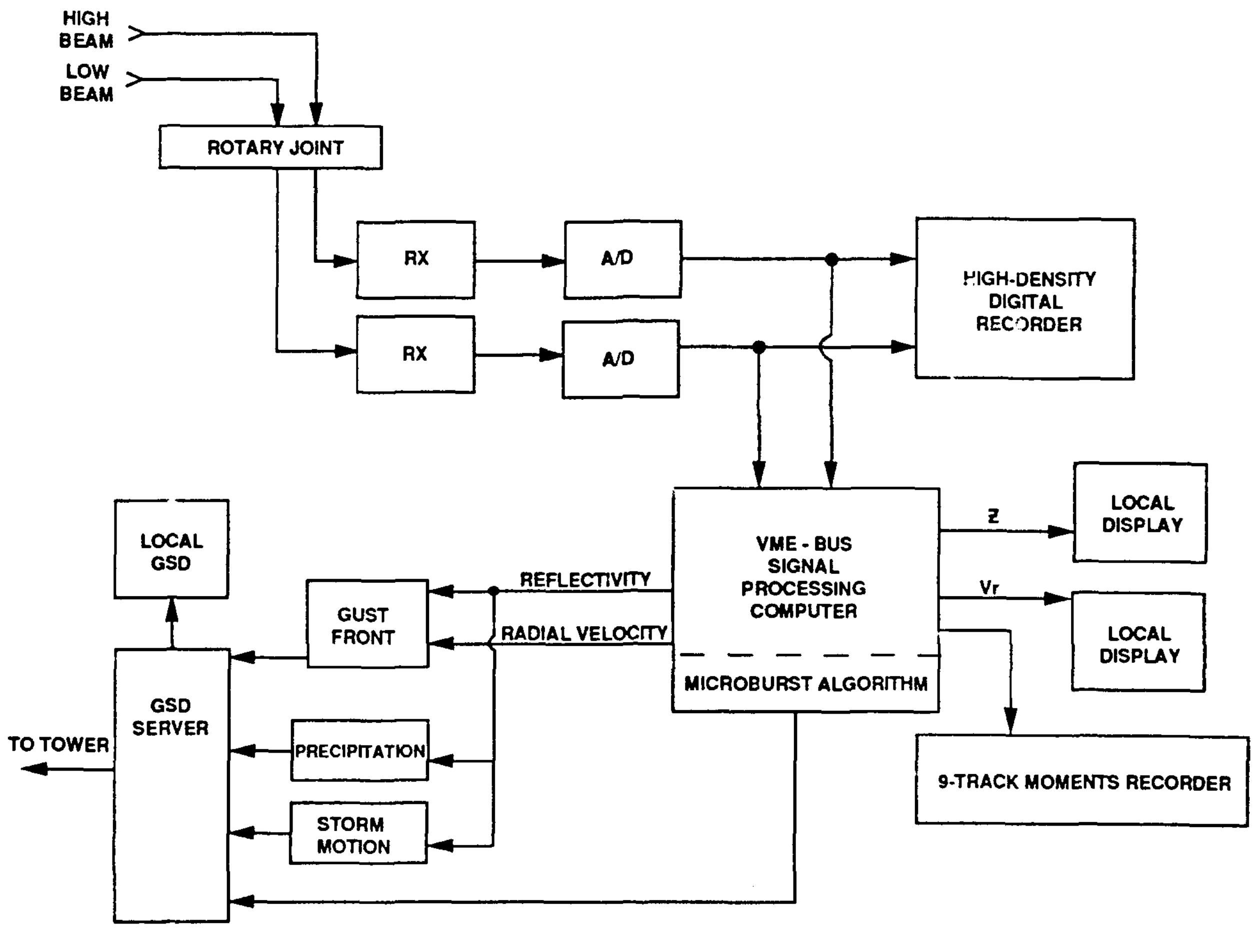

Figure 2: High-level block diagram of the 1990 Orlando ASR-WSP testbed processing and recording system.

Reflectivity and radial velocity estimates were passed to a distributed system of processors that implemented meteorological algorithms to detect microbursts and gust fronts and provide estimates of storm motion. The microburst detection algorithm was executed on a single-board computer in the same VME backplane as the array processor boards used for the signal processing. For convenience, gust front detection and storm motion tracking were performed on external workstations with Ethernet connections to the VME-bus processor. In a production implementation of an ASR-WSP, these external workstations could be replaced by additional single-board computers in order to minimize processor size and expense.

1.2.2. Meteorological Algorithms

A microburst is a sudden downburst of wind, which, upon impact with the ground, results in a divergent outflow. [4] The opposing horizontal components of velocity from the microburst are considered hazardous if they create a wind difference or shear which is greater than 10 m/s over a distance less than 4 km. An aircraft flying through a microburst encounters a lift-inducing headwind followed by a tailwind which causes air speed and altitude loss. A number of air carrier accidents have been attributed to this phenomenon. The ASR-WSP microburst algorithm detects this hazardous divergent outflow and generates microburst alerts within a 10 nmi radius.

Gust fronts are the boundary between the horizontally propagating cold air outflow from a thunderstorm and the surrounding environmental air. [5] Since an aircraft encountering a gust front experiences an increase in air speed, the tendency is towards greater lift; therefore, the large-scale wind shear associated with gust fronts is less hazardous than that associated with microbursts. However, turbulence and crosswinds associated with gust fronts can be hazardous. In addition, advanced warning of gust-front-induced wind shifts at an airport reduces delays associated with runway reconfiguration.

The ASR-WSP gust front algorithm used during the demonstration was based on detection of the "thin line" echo of enhanced reflectivity at the leading edge of gust fronts. Although this feature is not present in all gust fronts, prominent thin lines are frequently observed in association with strong gust fronts. Gust front detections were provided out to a range of 15 nmi for the 1990 operations. Ten- and 20-minute predicted locations, as well as expected wind shifts, were provided.

A discrete six-level precipitation product conforming to the National Weather Service (NWS) standard was also provided. This product is generated by thresholding the reflectivity measured by the low receiving beam of the ASR. A filled beam assumption was used in converting received power estimates to weather reflectivity.

The storm motion algorithm (SMA) uses a cross-correlation technique [6] to track the movement of existing storm cells. Storm motion is conveyed using a graphic vector labeled with the storm propagation speed. The intended use of the storm motion product is not for fine scale vectoring of aircraft, which would involve precision threading of aircraft through storm cells, but for aid in global vectoring decisions such as runway configuration selection. Storm motion was provided out to a range of 15 nmi during the 1990 operations.

1.2.3. Controller Products

ASR-WSP data were directly disseminated to controllers and supervisors using two types of displays. These displays are:

1. A ribbon (alphanumeric) display which shows wind shear hazard messages when LAWS impacts a runway safety corridor (defined below). These messages are relayed to pilots by air traffic controllers.
2. A geographical situation display (GSD) which presents weather data in a graphic format over the entire 15 nmi instrumented range to air traffic supervisors for planning purposes.

Microburst alarms from the ASR-WSP system were also overlaid on an off-line automated radar terminals system (ARTS) display in the Orlando TRACON by feeding in signals through its spare video port. When feasible, off-duty controllers and supervisors were asked to view this display and comment on its operational utility.

The ribbon display provided wind shear alerts in an alphanumeric format which did not require interpretation. The alert message described the affected runway, type of wind shear, the expected headwind change, and the location at which the wind shear would first be encountered along the runway corridor. The codes used on the display for alerts were: (1) MBA for microburst alert (wind shear with loss greater than 30 knots) and (2) WSA for wind shear alert (a wind shear alert with gain greater than 15 knots, or a wind shear alert with loss between 15 knots and 30 knots).

The operationally significant area was divided into two safety corridors, [7] depicted in Figure 3. The arrival safety corridor included the runway itself and three extensions along the runway centerline, reaching 1, 2 and 3 nmi from the runway end. The departure corridor included the departure runway and extensions of 1 and 2 nmi from the runway end. The safety corridors were defined to be 1 nmi wide about the extended runway centerline. Codes used on the display to indicate location were: (1) MF for miles final, (2) MD for miles departure, and (3) RWY for on the runway.

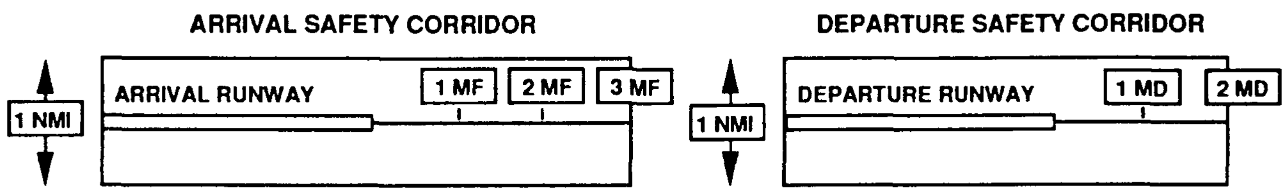

Figure 3: Safety corridors defining operationally significant area during Orlando 1990 demonstration.

When a microburst or gust front shape overlapped at least one rectangular region, an alert was issued for the location at which the wind shear would be first encountered by an aircraft. Alert messages were displayed along with the LLWAS center field and active runway threshold winds. Ribbon display terminals were located near the local and ground control positions in the Tower and near the supervisor's desk in the TRACON.

Graphic products from the ASR-WSP were presented on two separate color GSDs. One GSD was located at the supervisor's position in the Tower, and the other near the supervisor's position in the TRACON. Storm reflectivity information from the ASR-WSP was displayed on the GSD in the form of a graphical precipitation product, presented in the standard six-level NWS reflectivity scale.

The four other ASR-WSP products (microbursts, gust fronts, gust front predictions, and storm motion vectors) were also shown on these displays. Figure 4 shows the GSD monitor during a time of active weather. The microburst product is shown as a red circle. Note: an asymmetric microburst would be represented by a "bandaid," or rectangle with semicircular ends. The gust front is depicted as a purple curve, and the 10- and 20-minute predicted locations of the front are represented by dashed purple curves. The purple vector behind the front indicates the direction and magnitude in knots of the estimated winds behind the front. The storm motion product is represented by the blue vectors, which are labeled with an estimate of the storm propagation speed in knots.

Because the formats of the messages on both the alphanumeric ribbon displays and the GSDs were identical to those used during the preceding TDWR demonstration at MCO, no controller or supervisor training was required to use these devices.

1.3. THE VERIFICATION SYSTEM

Lincoln Laboratory's TDWR testbed, identified in Figure 1 as "FL-2C," provided independent measurements to support verification. FL-2C operates at C-band, with peak power of 250 kw, 120 m (1 μsec) range resolution and a 0.5-degree beamwidth. The radar's processor achieves 50 dB ground clutter suppression and utilizes extensive data quality control (i.e., clutter editing, point target filtering, second-trip weather censoring, velocity dealiasing) to ensure high-quality measurements of weather reflectivity and radial velocity. Meteorological "truth" derived from FL-2C reflectivity and velocity data was used for a quantitative measure of ASR-WSP performance for both the microburst and gust front detection functions.

Two additional Doppler weather radars, "UND" and "MIT" in Figure 1, were operated by the University of North Dakota and the Massachusetts Institute of Technology Weather Radar Laboratory, respectively. Both radars operate at C-band with range/azimuth resolutions of 120 meters/1.0 degree and 250 meters/1.4 degrees, respectively. Together, the three pencil beam Doppler weather radars provide complementary viewing angles for thunderstorm activity over MCO, allowing for triple-Doppler reconstruction of the full vector wind field. Data from all three radars will be used for future off-line dual- and triple-Doppler case studies of wind shear.

A network of 20 FAA-Lincoln Laboratory Operational Weather Studies (FLOWS) automatic weather stations (MESONETs) collected measurements of wind speed, wind direction, rainfall, temperature, humidity and pressure. The wind data from the MESONET and the local Low Level Wind Shear Alert System (LLWAS) stations, together with the pencil-beam radar data, may be used for additional validation of the wind shift detection capability of the testbed ASR-WSP. The data will support investigation of mechanisms for integrating ASR-WSP data with LLWAS data.

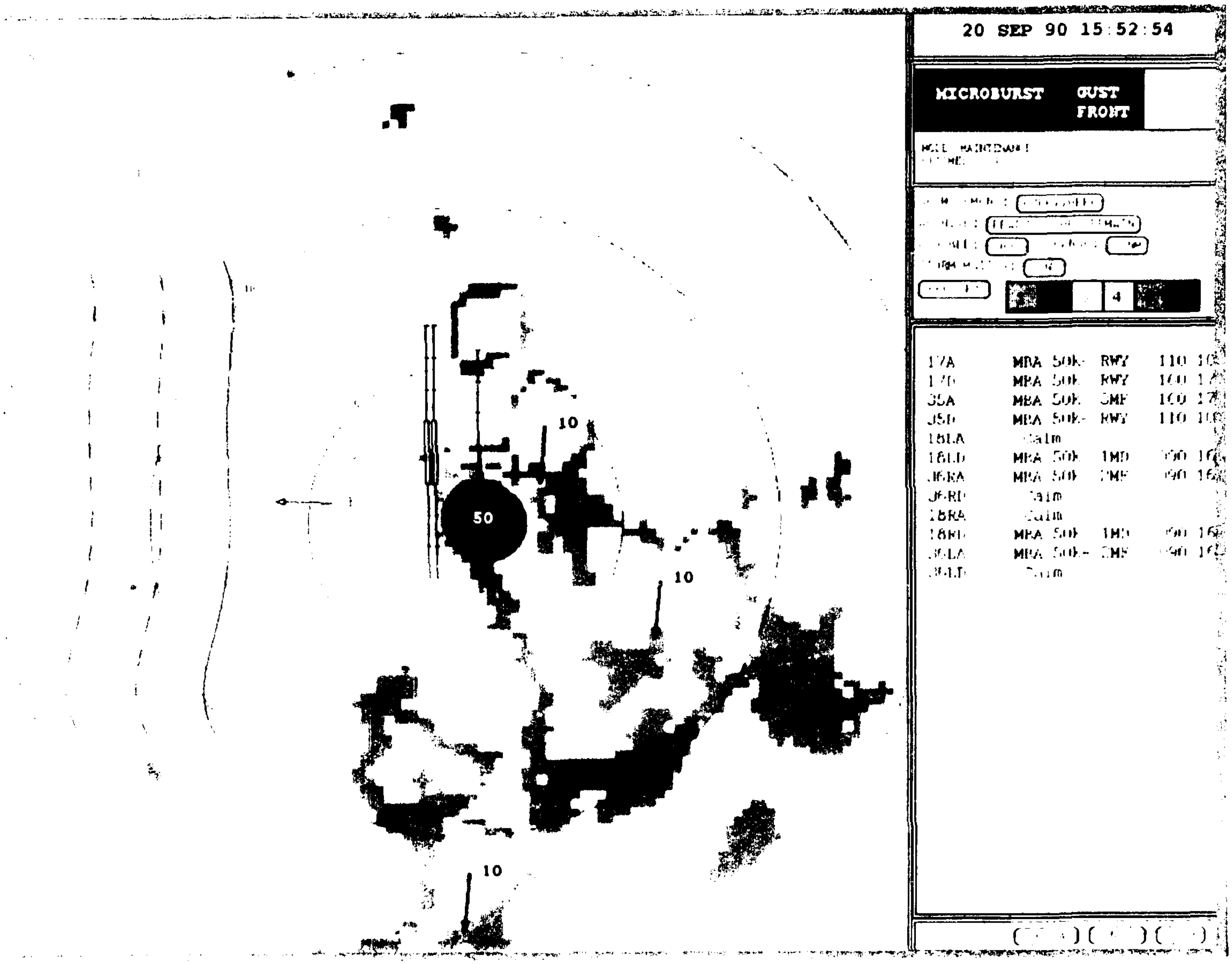

Figure 4: The Geographic Situation Display.

Lightning studies were conducted using a lightning interferometric detector, labeled "L" in Figure 1. This sensor, developed by ONERA of France, provides long-range location information on thunderstorm activity and is being used for studies which may provide insight into the development of storm cells and microburst activity.

1.4. SYNOPSIS OF WEATHER DURING OPERATIONS

Although September 1990 temperatures in the central Florida area averaged slightly (0 to 2 degrees C) above normal, dominant high pressure over the Southeastern United States suppressed convection; the month was classified as "extremely dry" by the NWS. During the first two weeks of September, expansive high-pressure cells in the upper atmosphere covered the entire Southern United States. Storms that developed in the Orlando area during the period were shallow and produced generally weak outflows (less than 18 m/s); the first weather activity at the airport occurred on September 11.

At mid-month, a weak cool front near the Florida/Georgia border triggered numerous showers in the moist air-mass ahead of the front. Microbursts as strong as 25 m/s were observed during activity on September 16 and 17. Upper-level low pressure over the eastern Gulf of Mexico at month's end produced a southwesterly flow of unstable air over the Orlando area. Showers and thunderstorms on September 28 and 29 produced numerous microburst and wind shear alerts near the airport.

Overall, radar reflectivities associated with microbursts during the operational test period were quite strong; all were greater than 40 dBZ, with a median of 50 dBZ. The ASR-WSP was able to detect the strong precipitation associated with these microbursts and was not subject to the sensitivity problem expected in "dry" environments such as the High Plains Region of the United States.

The majority of gust fronts were weak, with velocities less than 10 m/s. A reflectivity thin line was detected in three-quarters of the gust fronts. The reflectivity along the thin line varied from 0 to 30 dBZ, with a median of 10 dBZ.

Table 1 summarizes the weather activity at the airport during the operational period. Warnings and alerts issued by the microburst and gust front algorithms (those intersecting the runways or arrival and departure corridors) are included. Types of wind shear are signified by MB (microburst warning), WSA (wind shear with loss alert) and GF (gust front).

Table 1. Summary of Wind Shear Activity at Orlando International Airport During the 1990 ASR-WSP Operational Demonstration

DAY	TIME OF IMPACT ON AIRPORT (UT)	EVENT TYPE
AUG 30	21:00-21:21	GF
SEP 11	16:32-16:47 16:49-16:51 16:53-16:57	MB WSA WSA

SEP 16	17:16–17:27 17:20–17:22 17:20–17:27 17:22–17:26	MB WSA MB MB
SEP 17	20:37–21:22 20:50–20:56 20:53–20:56 21:32–21:37	GF WSA MB WSA
SEP 18	19:13–19:17	WSA
SEP 23	22:16–22:21	WSA
SEP 28	18:04–18:29 20:18–20:35 20:26–20:38 20:30–20:35 20:39–20:48 20:49–20:53 21:30–21:35 21:41–21:54 21:47–22:05 21:53–21:55	GF MB MB MB MB MB MB MB MB WSA
SEP 29	16:30–16:31 16:37–16:40 18:57–19:02 19:54–19:59	MB MB MB WSA

1.5. TEST PROCEDURES

The ASR–WSP was operational between the hours of 1600 and 2300 Z (12:00–7:00 pm EDT). Air traffic information systems (ATIS) messages released during this period contained the statement "Airport Surveillance Radar Wind Shear Detection Demonstration in Progress." Two Lincoln Laboratory observers were present -- one in the Tower cab and one in the TRACON -- to answer questions about the system and to assist in case of problems with display unit hardware or software. The display of six-station LLWAS winds in the Tower cab was covered, except for the centerfield wind readout.

Personnel from the FAA Technical Center acted as test monitors throughout the operational test period. They were stationed at the ASR–WSP site in order to simultaneously observe base data, algorithm products and user displays generated by the system.

1.6. TEST RESULTS

1.6.1. System Reliability

System down time due to hardware or software failures was minimal. A few brief (less than 10 minutes) interruptions in transmission of data occurred when:

1. The gust front association and discrimination module (ADM) faulted, resulting in interruption of the gust front algorithm data stream to the GSD. This problem was corrected largely through software changes to the gust front algorithm during the first week of testing;
2. Users entered inappropriate inputs to the GSD while attempting to change range scale or active runway configuration. This occurred on a number of occasions during the earlier TDWR test as well, indicating that controller familiarity with the GSD was insufficient and/or that the steps required for display reconfiguration were too difficult.

A motor generator failure at the ASR–WSP site on September 29 caused loss of power during a period of heavy thunderstorm activity. The site was switched to the alternate generator and the system was back on line within 20 minutes.

1.6.2. Base Data Generation Algorithms

Base data are the estimates of weather reflectivity and low–altitude radial velocity input to the meteorological algorithms. Those algorithms in turn generate wind shear and precipitation products on user displays. In three respects, Orlando was a favorable site for generating good quality base data:

1. Local ground clutter intensity was benign relative to previous ASR–WSP measurement sites (Huntsville, AL and Kansas City, KS). Intense clutter at Orlando was confined to a small area around the airport terminal buildings, hotels to the north of the airport, a few highway sections visible to the radar, and a tree line parallel to the shores of East Lake Tohopekaliga to the south;
2. Radar reflectivity associated with microburst wind shear was generally high, providing for good SNRs and SCRs. Bernella [1] shows that microburst outflow reflectivity distributions for Orlando exceed those from other measurement sites in the U.S.; and
3. The Orlando environment does not in general exhibit strong vertical shear in the ambient horizontal wind. This reduces the likelihood of erroneous low–altitude velocity estimates caused by a highly non–uniform vertical distribution of reflectivity and radial velocity.

The quality of base data estimates during the Orlando test allowed for high-confidence detection of microburst wind shear and for accurate portrayals of storm precipitation fields and storm motion estimates. Detection performance for low-reflectivity gust fronts, while operationally useful, was degraded by the absence of reliable measurements of gust front radial velocity convergence.

Base data quality issues dentified during the operational test are listed below:

1. Temperature/humidity profiles conducive to anomalous propagation (AP) of radio frequency energy are frequent in Orlando. This condition can produce false weather echoes caused by ground clutter in areas that are normally free of clutter (and therefore not flagged in the processor's ground clutter maps). This has been a concern for usage of weather channel data from the operational ASR-9 in Orlando. Occasional breakthrough of AP-generated ground clutter caused some false precipitation regions to be displayed on the ASR-WSP GSD. Initially, the gust front algorithm generated a few false thin line features in regions of AP-generated clutter. This problem was corrected by requiring that the mean Doppler velocity associated with detected thin line features be non-zero.

   Doppler processing allows for discrimination between AP and true weather echoes based on the spectral characteristics of the echo. An algorithm for censoring of AP-generated clutter is being evaluated off-line. If its performance is acceptable, AP censoring will be implemented during the 1991 ASR-WSP demonstration.

2. Second-trip weather echoes generally extend much farther in range than in azimuth. These echoes can be very similar to gust front thin lines and initially resulted in some false gust front detections. This problem was greatly alleviated by modifying the algorithm to reject radially-oriented thin line features. Because real gust fronts may become radially oriented as they pass over the radar, the gust front algorithm employed temporal continuity logic to track true gust fronts as they pass overhead.

1.6.3. Microburst Algorithm Performance

Microburst activity near Orlando International airport occurred on only seven days during the operational test period. As stated previously, many of these events were weak (15 to 40 knots maximum loss) and were associated with shallow rainshowers and thunderstorms. In order to augment the data set used for "scoring" of microburst algorithm performance, we have included all data from the week preceding the start of the ASR-WSP test (August 22 through 29). This period included two days of thunderstorm activity and a number of strong microbursts on the airport.

Table 2 summarizes detection and false alarm probabilities for the microburst algorithm. Data included in the study, as well as procedures used to generate comparison "truth" and to perform the scoring, are described in Section 3.

Table 2. Microburst Detection Algorithm Performance

	> 10 m/s	> 15 m/s	> 20 m/s
Probability of Detection	**0.84**	**0.97**	**0.98**
Probability of False Alarm	**0.16**	**0.10**	**0.00**

The detection probabilities for moderate to strong microbursts (greater than 15 m/s measured loss) are consistent with previous analyses of ASR–WSP performance in the southeastern United States, [2,3] indicating that the high–reflectivity outflows characteristic of this environment can be reliably detected. Detection probabilities for weaker microbursts or "wind shear alerts" were significantly lower. Initial analysis indicates that many of these missed detections for weak microbursts resulted when the ASR–WSPs divergence estimates were slightly lower than those from TDWR "truth." In some cases, asymmetry in the outflow strength contributed to loss estimate discrepancies between the two radars since the respective aspect angles were often quite different.

False–alarm probabilities were acceptable, although higher than expected from earlier measurements. The majority of the false microburst declarations occurred during brief periods of strong, gusty winds and heavy rain on the last two weather days of the test. Airport operations during these periods were curtailed owing to the wind and heavy rain. Section 3 contains specific examples of missed detections and false alarms for the microburst algorithm.

1.6.4. Gust Front Detection Performance

As stated earlier, the ASR–WSP gust front algorithm used during the demonstration was based on detection of the "thin line" echo of enhanced reflectivity at the gust front's leading edge. Although this feature is not present in all gust fronts, prominent thin lines are frequently observed in association with strong gust fronts.

In spite of the limited weather activity during the operational period, the algorithm successfully identified 15 gust fronts. Although a number of false gust front detections were generated during the test period, none of these impacted the airport runways or caused an alert to be generated.

Section 4 presents an analysis of gust front algorithm performance for moderate and strong gust fronts. The analysis considers gust fronts with velocity shear of 10 m/s or greater that passed over the Orlando airport. Since only one such event occurred during the operational test period, the data set for the study was expanded to include all such gust fronts observed during the three–month period that the ASR–WSP collected data in Orlando.

Of the seven airport-impacting moderate to strong gust fronts during this period, four were detected by the algorithm. The three gust fronts missed by the algorithm did not produce discernible thin line features in the ASR-WSP reflectivity field. While the one strong gust front that occurred during the operational test period was detected well in advance of its arrival at the airport, the remaining three detected fronts in the analyzed data set did not move out ahead of the generating storm and form a thin line until after the storm had passed over the airport.

1.6.5. Storm Motion Algorithm Performance

Performance of the storm motion algorithm has been quantitatively assessed by Chornoboy [6] using TDWR testbed data from Denver and Kansas City. Errors in the estimates of storm advection speed and direction are related to the uncertainty in scan-to-scan displacement estimates. These in turn depend largely on the pixel size of the reflectivity images and the time interval between successive images that are cross-correlated. Using a 1 km pixel size and a five-minute interscan interval, Chornoboy found that for storms moving faster than 10 knots, errors in the estimated direction of motion were less than 30 degrees; this error increases rapidly for storms moving more slowly. Mean error in the estimated speed of advection was three knots, independent of storm advection speed.

Both the reflectivity image pixel size and the interval between successive images were halved when the storm motion algorithm was implemented for the ASR-WSP. The above error estimates should therefore remain valid. Observations of the ASR-WSP storm motion estimates during the test period confirmed that the algorithm estimates were accurate and consistent for fast moving storms. Direction estimates for storms with advection speeds of less than 10 knots were less accurate and often fluctuated by as much as 90 degrees over relatively short time intervals. Storms on the edge of the 15 nmi range of data processed also were not well tracked in some cases because the artificial "zeroing" of reflectivity at greater ranges distorted the scan-to-scan correlation function used to determine displacement vectors.

1.6.6. Air Traffic Controller and Supervisor Assessment

The FAA Technical Center distributed questionnaires on the ASR-WSP system to all Orlando air traffic controllers and supervisors at the conclusion of the test period. The ATC personnel were asked to rate various aspects of the system and to respond to specific questions on the usefulness of the ASR-WSP. Forty-nine controllers responded, although many respondents did not answer all the questions. Some controllers indicated that they had not been able to assess all aspects of the system owing to the lack of severe weather during their on-duty time.

Table 3 summarizes user responses to four key questions. Summary responses for the other questions and individual controller comments on the various questions asked are given in Section 6. Overall, user response to the ASR-WSP as assessed by the numerical ratings was favorable. About 80 percent of the respondents indicated that the benefits associated with the system exceeded its problems and that it helped them in their job of controlling local traffic. Approximately 85 percent responded that the system was suitable for widespread operational deployment, although most indicated that adjustments and/or changes would be beneficial.

Table 3. Air Traffic Controller Responses to Questionnaire

ITEM BEING EVALUATED	RATING SCALE							
	-3	-2	-1	0	1	2	3	?
Do you see the ASR-WSP as a help or a hindrance to your job of controlling local traffic?	1	3	4	0	4	16	9	1
Do you see the ASR-WSP as a help or a hindrance to the pilot?	0	0	1	0	3	24	10	0
Please rate the relative magnitude of the benefits and problems of the ASR-WSP.	1	1	1	5	5	17	7	0
Based on your present knowledge, please rate the ASR-WSP's suitability for widespread operational use in the field.	0	1	1	3	12	17	3	2

Individual comments raised a number of concerns also voiced to Lincoln Laboratory observers during the test period. A recurrent complaint was that the microburst product sometimes severely impeded traffic flow in situations where the controllers felt they could have safely worked around or through the weather. A number of respondents stated the concern that "false alarms must be minimal" if the system is to provide benefits. Because of runway buffer zones, the relatively coarse locational information relayed to pilots in the microburst messages, and the rapid vertical variation in microburst outflow strength, airplanes that choose to continue a landing or takeoff when an alert is in effect may not encounter the indicated shear, even when the alarm reflects an accurate detection of wind shear. Pilot reports of such discrepancies reduce controller confidence in the validity of alarms.

Several comments indicated that the imprecise locational information provided by alphanumeric messages on the RDTs was a concern. One respondent commented that there should be "a GSD for each position in the Tower and at least 5 or 6 in the TRACON." Several controllers stated that displays showing wind shear locations should be uplinked directly to aircraft who could then make an informed decision as to whether a takeoff or landing was safe. Research is underway to develop a cockpit display of wind shear information. [8]

Use of the term "microburst alert" was flagged as a "scare tactic" both in questionnaire responses and in statements by controllers and supervisors to the Lincoln Laboratory observers. It was suggested that a better procedure would be to always issue the messages as "wind shear alert" and allow the stated loss value to convey the severity of the event.

Display of microburst alerts on the ARTS display was viewed as a useful feature. However, several controller comments confirmed the impression of Lincoln Laboratory observers that the microburst shapes were difficult to see when superimposed on the aircraft tags, maps and weather information already on the ARTS. It was also apparent that a better assessment of the utility of ARTS display of windshear information would be obtained by providing the display at working TRACON positions such as final and departure controllers.

The gust front prediction product, color display of six-level storm intensity and storm motion products were received favorably. All of these products provide advisory information to be used at the discretion of the controllers or supervisors. Several comments emphasized the value of advanced prediction of wind shifts.

1.7. SUMMARY AND RECOMMENDATIONS

This first operational evaluation of an ASR-WSP provided a valuable opportunity to test the system over an extended period of continuous operations (seven hours per day, seven days per week) and to obtain feedback from air traffic controllers and supervisors on the strengths and weaknesses of the system. Although thunderstorm activity was less frequent than anticipated, weather activity was sufficient to allow many of the Orlando controllers to work with the system. Better statistical confidence in quantitative analysis of the performance of the wind shear detection algorithms was obtained by extending the data set to include weather data recorded by the ASR-WSP prior to its operational test period.

System performance was generally consistent with previous, off-line evaluations of ASR-based wind shear detection capability in the southeastern United States. The capability to reliably detect strong microbursts was confirmed. The initial implementation of a gust front detection algorithm based on "thin line" detection allowed for detection of slightly more than half of the moderate and strong gust fronts observed during the Orlando measurement period. This is consistent with previous analyses of gust fronts in Huntsville, AL and Kansas City, KS, indicating that the ASR measures well-defined thin lines in about half of the fronts.

Orlando air traffic controllers and their supervisors provided a generally favorable assessment of the system. During periods when weather impacted airport operations, the Lincoln Laboratory observers in the tower noted intense interest by controllers and supervisors in the information being presented on the GSD. Many controllers, however, voiced concerns that algorithms and procedures should be perfected so as to minimize unnecessary delays. It was clear from their comments that the sense of microburst "overwarning" that arose during the preceding TDWR test persisted through the ASR-WSP test. The value of advanced warnings of wind shifts due to thunderstorm-generated gust fronts was echoed by several controllers.

Overall, the operational test established that a wind shear modification to the ASR-9 could enhance the safety and efficiency of air traffic operations, either in a stand-alone mode or integrated with dedicated sensors such as TDWR or enhanced LLWAS. Ongoing system and algorithm refinements, as described in the remaining sections of this report, will provide improved performance directly addressing many of the concerns raised by controller comments. Specifically:

1. The signal processing hardware used by the ASR-WSP is being upgraded to allow for implementation of more advanced algorithms for low-altitude radial velocity measurement. More accurate velocity measurements will improve the ability of the system to detect weak microbursts (wind shear alerts) and will reduce the incidence of erroneous wind shear and microburst alerts;

2. The processor upgrade and receiver modifications will also allow for improved measurements of radial velocity under low SNR conditions, as at the leading edge of a gust front. Detection of radial convergence associated with gust fronts, in addition to their thin lines, should significantly improve the capability to generate wind shift warnings;
3. The gust front detection algorithm is being refined to provide better thin line detection and to incorporate radial velocity convergence features, where available, in the detection process; and
4. The microburst algorithm output module is being modified to provide more frequent updating of microburst alarms.

Additional operational testing of the ASR–WSP in Orlando is planned for the summer of 1991. This will be conducted using a production ASR–9, suitably modified so as to provide wind shear detection capability without impact on the radar's primary function of aircraft detection and tracking. In contrast to the 1990 operational test, the 1991 test period will coincide with the months of peak thunderstorm activity in Florida (June, July and August).

1.8. SCOPE OF REMAINDER OF REPORT

The remainder of this report is broken down into five sections. Section 2 provides a description of the 1990 ASR–WSP system configuration and signal processing algorithms. Sections 3 through 5 describe the microburst, gust front, and storm motion products, respectively.

Section 6 provides responses to the questionnaire distributed to Orlando Air Traffic personnel following the 1990 demonstration.

2. 1990 ASR-WSP SYSTEM CONFIGURATION

The functional block diagram of Figure 2 (page 5) shows the major components of the 1990 ASR-WSP system. This section provides a description of the signal processing computer (labeled "VME-BUS SIGNAL PROCESSING COMPUTER" in Figure 2) and the signal processing algorithms used to generate polar reflectivity and velocity fields from in-phase and quadrature (IQ) data.

2.1. SIGNAL PROCESSING HARDWARE

The 1990 ASR-WSP signal processor consists of seven Mercury Computer (MC) processors; six processors perform the actual signal processing and one processor is dedicated to managing the distribution of the input data stream. The design also incorporates several computer systems connected by both proprietary and VME buses (see Figure 5). The system operates as a loosely coupled multiprocessor. The input processor receives a 10-megabyte-per-second data stream from the radar. After receiving the data from each transmitted pulse, it forms a message for each of the six signal processing boards. Each of the signal processors is dedicated to processing the data for a specific range of distances from the radar and only receives the data for that area. The data is managed using ring buffers in the memories of the signal processors that are loaded by the input processor and are read by the signal processors. The messages are transferred to the signal processing boards using MC to MC VME-bus block-mode transfers at 24 megabytes per second. Control information is passed into the signal processors using the same ring buffer mechanism.

Each signal processor runs a single task that continuously inspects the on-board ring buffers for input data. When the buffer contains enough data for the processor to run the signal processing algorithms, the data is transferred out of the ring buffers and processed. Meanwhile, the input processor can continue to place fresh data in the ring buffer without interrupting the signal processor's activity, with the exception of the time penalty for off-board accesses to the processor's memory. A combination of calls to the Mercury Scientific Algorithm Library (SAL) and microcoded routines are used to perform the high-pass filtering, auto-correlation, and median filtering functions.

The reflectivity and velocity information generated by each signal processor board is placed in another on-board ring buffer dedicated to holding the output data. A 68030-based single-board computer retrieves the output data from the output ring buffers of all the signal processing boards. It assembles the output data to form the reflectivity and velocity maps which are then passed on to the algorithm processors. Utilizing the ring buffer scheme completely isolates the signal processing boards from the input and output interfaces. It also allows the signal processing boards to spend their time doing signal processing instead of interface management.

2.2. SIGNAL PROCESSING ALGORITHMS

Figure 6 diagrams the signal processing flow used during the operational test period in 1990. Incoming time-series data for the high and low beams are processed in 26-sample

blocks which consist of one eight-pulse (low PRF) coherent processing interval (CPI), one ten-pulse (high PRF) CPI, and a final eight-pulse CPI. Thus, the data processing interval spans 1.5 antenna beamwidths and successive intervals are overlapped by 50 percent. This extended CPI provides the longest available "deterministic" waveform and allows for cell-by-cell selection of the level of clutter suppression.

For each resolution cell, a map stores clutter residue power out of three 17-point finite impulse response (FIR) filters and an all-pass filter. The clutter filter used in processing is the least attenuating of these filters that maintains signal-to-(stored)clutter residue power in excess of a threshold, which is set at 10 dB. A "bad data" flag is set for resolution cells where the most attenuating filter output does not exceed this threshold. The FIR filter coefficients are programmed to vary from pulse-to-pulse in order to accomplish data interpolation.

Zero- and one-sample-delay autocorrelation lag estimates are computed for both beams, SNR is calculated, and data are flagged as "bad" if the SNR is less than a threshold (currently 7 dB). Radial velocity is computed using one of two algorithms, with the selection based on the results of the SNR test. If only the high-beam signal fails the SNR test -- typically the case, for example, in gust front thin lines -- the velocity is computed as the phase angle of the low-beam R(1) estimate. If both beams pass the SNR test, the velocity is estimated using a function that combines the low- and high-beam R(0) and R(1) estimates to cancel signal contributions not associated with near-surface scattering. Reflectivity is calculated using the low-beam R(0) estimate.

Spatial filtering is identical for the reflectivity and radial velocity fields and is implemented in two stages. A 3 x 3 median filter is followed by a five-point Gaussian-shaped filter applied along the range axis. Temporal filtering of the reflectivity field is implemented as a six-scan moving average; for the velocity field, a single-pole infinite impulse response (IIR) filter with feedback coefficient of 0.5 is used.

The data streams passed to the algorithms therefore consist of one reflectivity and one radial velocity field, with "bad value" flags (and no moments estimates) inserted for resolution cells exhibiting low SNR or low SCR.

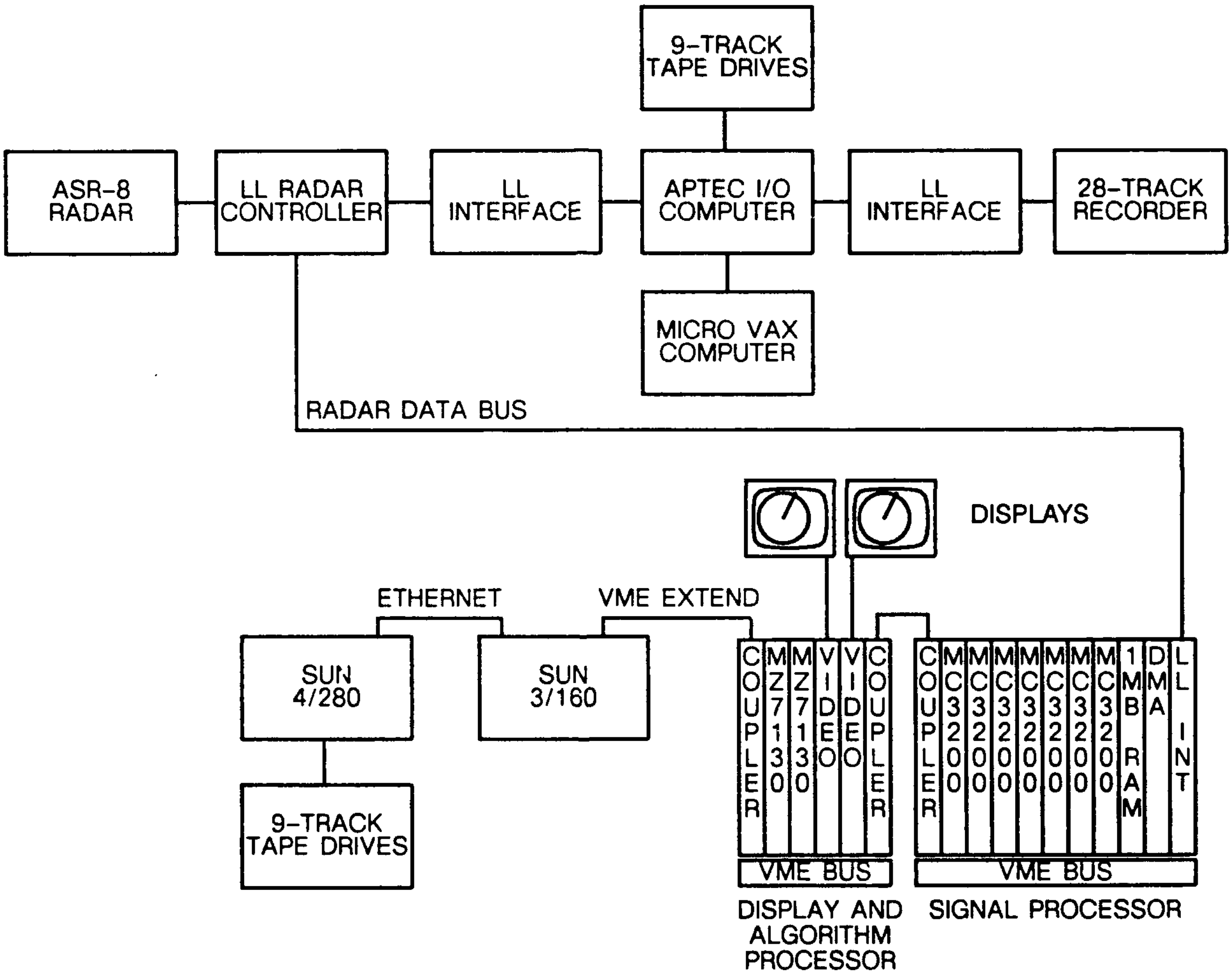

Figure 5. 1990 ASR-WSP Signal Processor Configuration

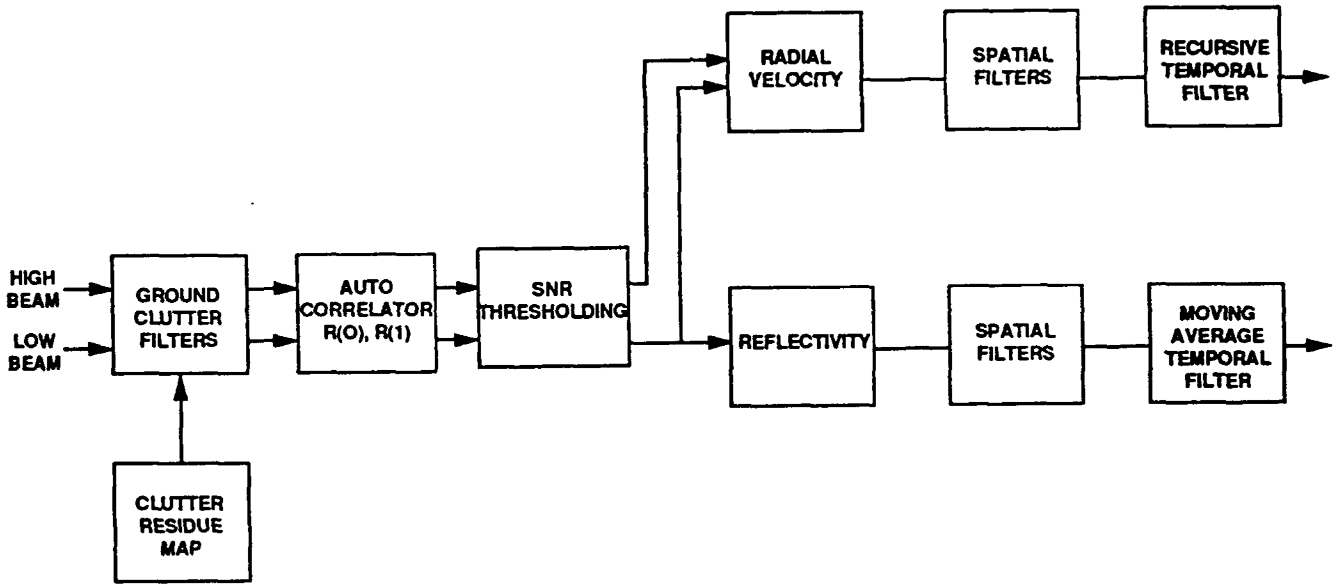

Figure 6: 1990 ASR–WSP Signal Processing Algorithms.

2.3. PROPOSED MODIFICATIONS

Based on results of the 1990 testing, modifications are being made to the ASR–WSP to accomplish the following:

1. Support better quality velocity estimates by means of spatial and temporal averaging of the autocorrelation estimates;
2. Allow the meteorological detection algorithms to decide independently whether to use or discard the reflectivity and radial velocity data based on SNR and the presence of censor flags; and
3. Provide a framework within which data quality algorithms can be implemented to detect conditions such as second trip weather, velocity unfolding, anomalous propagation and low SCR.

3. MICROBURST DETECTION ALGORITHM

3.1. ALGORITHM DESCRIPTION

Low-level wind shear originating from a microburst outflow produces a run of radial velocities that are generally increasing with radar range, corresponding to a transition from approaching winds on the near side of the downdraft core to receding winds on the far side of the downdraft. To be considered hazardous, the velocity increase, or "shear," must exceed 15 knots over a distance of not more than 2 nmi. This signature is shown graphically in Figure 7. Runs of velocities that meet these criteria are termed shear "segments," and are the basic building blocks used to produce microburst alarms and wind shear alerts.

The microburst detection algorithm currently employed in the ASR-WSP is an adaptation of the 1987 TDWR Microburst Detection Algorithm [9] designed to run efficiently within the ASR-WSP architecture. Spatial smoothing of the radar data prior to execution of the ASR-WSP microburst algorithm allows an approach that is less noise-tolerant than the TDWR algorithm. The reduced complexity allows the algorithm to run at real-time rates (4.8 seconds per scan) on a single-board computer. A dedicated MIZAR CPU is used in the current ASR-WSP system.

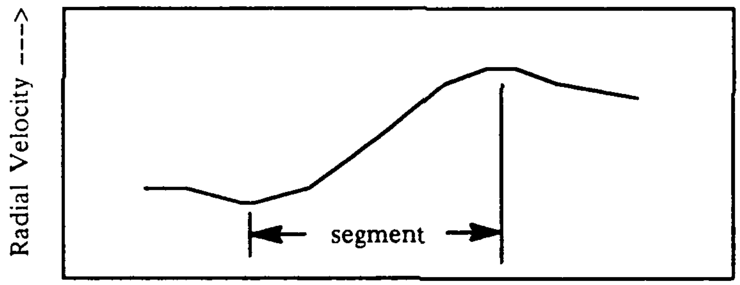

Figure 7. Shear Segment Signature

The algorithm is composed of three major steps: shear segment identification, shear segment association, and temporal smoothing. A brief description of each step is provided below. In addition, algorithm parameters used during the operational test are listed in Table 4 at the end of this section.

3.1.1. Shear Segment Identification

The four major steps used to detect shear segments on an individual scan are:

1. Search for an initial gate-to-gate velocity increase, signifying the start of a candidate shear segment.
2. Grow the segment until a decreasing velocity pattern is detected. The segment is terminated when the sum of the velocity decreases relative to the maximum velocity in the segment reaches 5.0 m/s.

3. Apply a slope threshold to the segment and edit out areas of insufficient shear. The slope at a point is determined to be the larger of the two values calculated using a least-squares linear fit to the data within a seven-gate (0.84 km) and an 11-gate (1.32 km) window, respectively. At the segment ends, the window size is reduced to fit within the segment end points. Areas of a segment with a slope less than a minimum (2.5 m/s/km) are eliminated.
4. Apply segment wind speed loss and length thresholds. To be considered valid, a segment must exhibit a differential velocity of at least 7.5 m/s and a length of at least eight radar range gates (0.96 km).

3.1.2. Shear Segment Association

Once shear segments have been produced for a scan, they are associated into wind shear with loss alerts (7.5 to 14.9 m/s) and microburst alarms (greater than 15 m/s). This is accomplished by grouping shear segments that overlap in range and are within a given azimuthal distance. An example of the association process is shown in Figure 8.

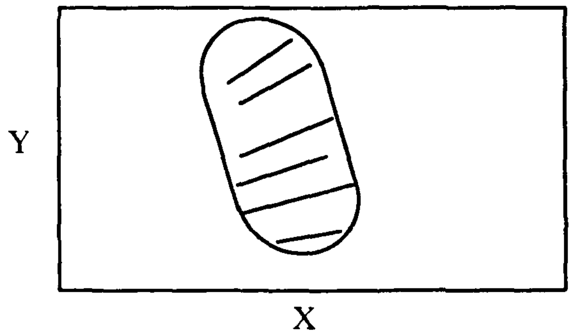

Figure 8. Shear Segment Association

The association is performed using two passes through the list of shear segments -- the first pass to generate the microburst alarms, and the second to generate the wind shear with loss alerts. The two-pass method allows different grouping parameters to be used for the two different strength categories, which provides added flexibility when tuning the parameters.

Regions formed by the grouping process must meet further area, wind speed loss, and associated reflectivity requirements before being passed on to the temporal smoothing stage of the algorithm.

Regions meeting the wind speed loss and area requirements (specified in the parameter list of Table 4) are subjected to a reflectivity criterion. The reflectivity association logic requires 40 percent of the region area to be greater than an adaptive reflectivity threshold computed for the scan.

3.1.3. Temporal Smoothing of Alerts and Alarms

To reduce short-duration false warnings and to enhance the continuity of valid warnings, temporal smoothing is performed. An alarm or alert must appear on three succes-

sive scans (15 seconds) in order to become valid, and once valid must be absent for six consecutive scans (30 seconds) before being eliminated. These settings were derived based on evaluation of data collected in Orlando prior to the operational test.

Table 4. Microburst Detection Algorithm Parameters

PARAMETER NAME	DESCRIPTION	SETTING
MAX_SUM_DECREASES	Sum of velocity decreases required for segment termination.	5.0 m/s
MIN_SEG_SLOPE	Minimum slope required over any portion of shear segment.	2.5 m/s/km
MIN_SEG_DV	Minimum required differential velocity across segment.	7.5 m/s
MIN_SEG_LENGTH	Minimum required segment length.	.96 km
MIN_ALERT_STRENGTH	Minimum wind speed loss required for a wind shear with loss alert.	7.5 m/s
MIN_ALERT_AREA	Minimum area required for a wind shear with loss alert.	2.8 km^2
MIN_ALARM_STRENGTH	Minimum wind speed loss required for a microburst alarm.	15.0 m/s
MIN_ALARM_AREA	Minimum area required for a microburst alarm.	2.0 km^2
MIN_REF_THRESH	Minimum bound on the value of reflectivity threshold.	30 dBZ
MIN_TIME	Minimum time required for valid alert/alarm.	15 seconds
MAX_COAST_TIME	Maximum alarm/alert coast time.	30 seconds

3.2. ALGORITHM PERFORMANCE

An assessment of microburst algorithm performance in Orlando was obtained by scoring algorithm output from five active days during the operational demonstration period and two additional days prior to the demonstration period. A summary of microburst activity during the scored periods is provided in Table 5.

Table 5. Summary of Microburst Activity on Days Scored

DATE	TIME PERIOD SCORED (UT)	NUMBER OF EVENTS WITHIN 20 KM OF ASR	MAXIMUM VELOCITY DIFFERENTIAL OBSERVED (m/s)
August 22	2020–2120	8	33
August 27	1847–2020	10	30
August 30	2112–2138	2	14
September 11	1604–1721	5	17
September 16	1708–1742	4	14
September 17	2023–2201	15	26
September 28	2028–2154	10	24

3.2.1. Scoring Method

Algorithm outputs were scored against surface "truth" derived from data collected by the TDWR testbed radar, located approximately eight kilometers south of the ASR-WSP ("FL-2C" in Figure 1, Page 3). Truth polygons indicating the location and extent of microbursts within 20 km of the ASR-WSP were generated by trained meteorologists upon examination of reflectivity and velocity estimates from the TDWR testbed.

The automated scoring process applied the following rules:

1. A microburst was considered "detected" if its truth polygon was intersected by one or more algorithm alarms.
2. An algorithm alarm was considered "false" if it did not intersect a truth polygon.

The two metrics used to measure (or "score") algorithm performance were:

Probability of Detection (POD) - The number of detected microbursts divided by the total number of microbursts.

Probability of False Alarm (PFA) - The number of algorithm alarms not associated with valid microbursts (false alarms) divided by the total number of alarms issued by the algorithm.

3.2.2. Scoring Results

All ASR scans within 30 seconds of an FL-2C scan were scored. The results of the scoring for events within four different range categories of the ASR are shown in Table 6. Note that for the Probability of Detection, the table utilizes the strength category of the truth event, and for the Probability of False Alarm metric, the table utilizes the strength of the algorithm alarm.

Table 6. Microburst Algorithm Scoring Results

0 < RANGE < 4 km				
ΔV_R	>= 10 m/s	>= 15 m/s	>= 20 m/s	>= 25 m/s
POD	0.82	0.97	0.97	1.00
PFA	0.00	0.00	0.00	0.00
0 < RANGE < 8 km				
ΔV_R	>= 10 m/s	>= 15 m/s	>= 20 m/s	>= 25 m/s
POD	0.84	0.97	0.98	1.00
PFA	0.16	0.10	0.00	0.00

0 < RANGE < 12 km				
ΔV_R	>= 10 m/s	>= 15 m/s	>= 20 m/s	>= 25 m/s
POD	0.81	0.92	0.93	1.00
PFA	0.25	0.13	0.03	0.00
0 < RANGE < 16 km				
ΔV_R	>= 10 m/s	>= 15 m/s	>= 20 m/s	>= 25 m/s
POD	0.79	0.90	0.93	1.00
PFA	0.28	0.13	0.02	0.00

The Probability of Detection and Probability of False Alarm values for microburst alarm strength events (15 m/s or stronger) on the airport (within 8 km of the ASR) satisfy the 0.9/0.1 limits prescribed by the FAA's TDWR System Requirements Statement. The probability of detecting an event increases as the event strength increases, and the probability an alarm is false decreases with increased alarm strength, for all range categories.

Although performance drops off as the range from the radar increases, it is still close to meeting operational requirements all the way out to 16 km; this suggests a possible operational utility at longer range.

3.2.3. Examples of Missed Detections and False Alarms

We have analyzed specific cases of false microburst alarms or missed detections generated by the ASR–WSP to understand the circumstances that produced them. As shown by the statistics in the previous subsection and in the following examples, these occur primarily in the weaker shear categories. The following three examples give a sense of the nature of these false alarms or missed detections. In Figures 9 through 11, segments and alarms generated by the microburst algorithm are shown in white, and FL-2C truth boxes are shown in red.

Figure 9 is an example of a false alarm produced by a non-uniform distribution of reflectivity in the vertical. The alarm box centered at 5 km, 15 degrees from the ASR (upper left window), corresponds to the region 13 km, 10 degrees from the TDWR tested (upper right). A synthesized range–height indicator (RHI) scan through this region indicates that at 12 km range from the ASR, precipitation reflectivity was significantly higher aloft than at the surface. As a result, the ASR measured the negative velocities at 1 to 2 km altitude rather than the positive radial winds observed by the TDWR at the surface. At a slightly greater range, there was a region of heavier rain at the surface so that the ASR measured the positive near–surface winds. The effect of this structure was to produce a larger divergence estimate (15 m/s) from the ASR than was observed in the same region by TDWR (9 m/s). This is therefore classified as a false alarm.

Figure 10 is an example of a microburst missed detection caused by area thresholds utilized by the microburst detection algorithm. The red polygons indicate the locations

of microbursts observed by the truth radar. FL-2C data appears in the bottom windows. Divergence segments were detected in the ASR velocity field near 5 km, 180 degrees (upper right), but the area of the polygon surrounding the segments was only 2.5 square km, shy of the 2.8 square km required by the algorithm for shear regions of less than 15 m/s velocity differential.

A microburst missed detection caused by algorithm segment association rules is shown in Figure 11. The cluster of shear segments found by the algorithm near 7 km, 245 degrees (upper windows) was not associated with the cluster found at 4 km, 260 degrees because of an "overlap" rule that permits association only if a segment detected along an adjacent radial lies at least 50 percent alongside the neighboring segment. Thus, the two clusters were considered separate shear regions with areas of 1.5 and 1.9 square km, respectively, and both failed the 2.8-square km area requirement. Corresponding FL-2C data is shown in bottom windows.

To summarize, ASR-WSP generated microburst false alarms and missed detections can be attributed to a few factors. False alarms were most often caused by velocity estimate inaccuracies due to overhanging precipitation or other variable vertical storm structures. In addition, the combination of microburst asymmetry and large viewing angle discrepancy between the truth radar and ASR-WSP could result in a large velocity discrepancy between the two data sets and therefore cause a false alarm or missed detection. Algorithm logic, and in particular fixed area thresholding and segment association rules, can cause missed microburst detections.

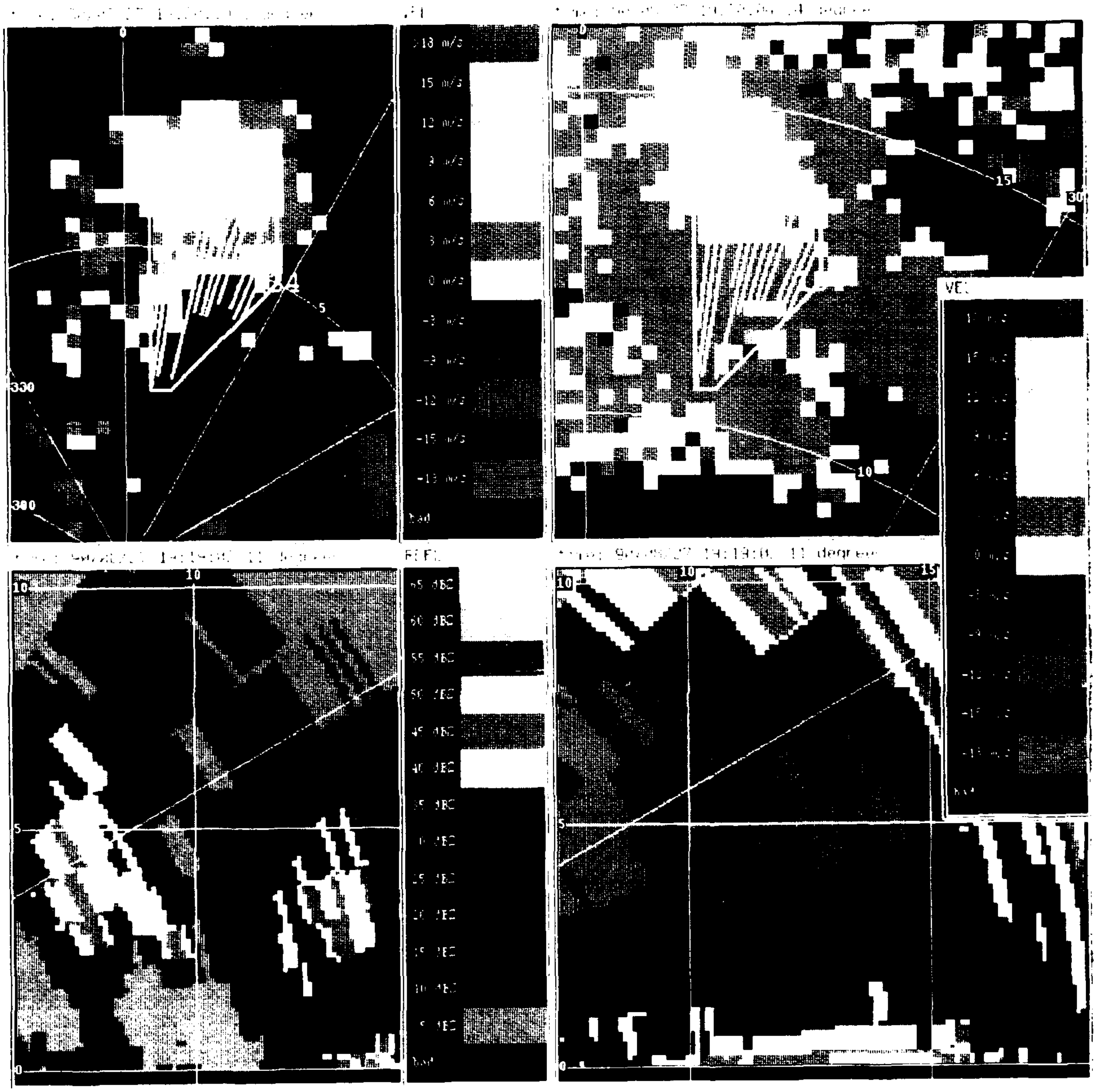

Figure 9. False Alarm Produced by an Elevated Reflectivity Core. Upper left: Alarm generated by ASR-WSP at 5 km, 15 degrees; Upper right: Corresponding truth region at 13 km, 10 degrees from truth radar; Lower Left: Synthesized RHI derived from truth radar data showing overhanging precipitation at 12 km range (4 km from ASR-WSP); Lower right: Velocity data from synthesized RHI

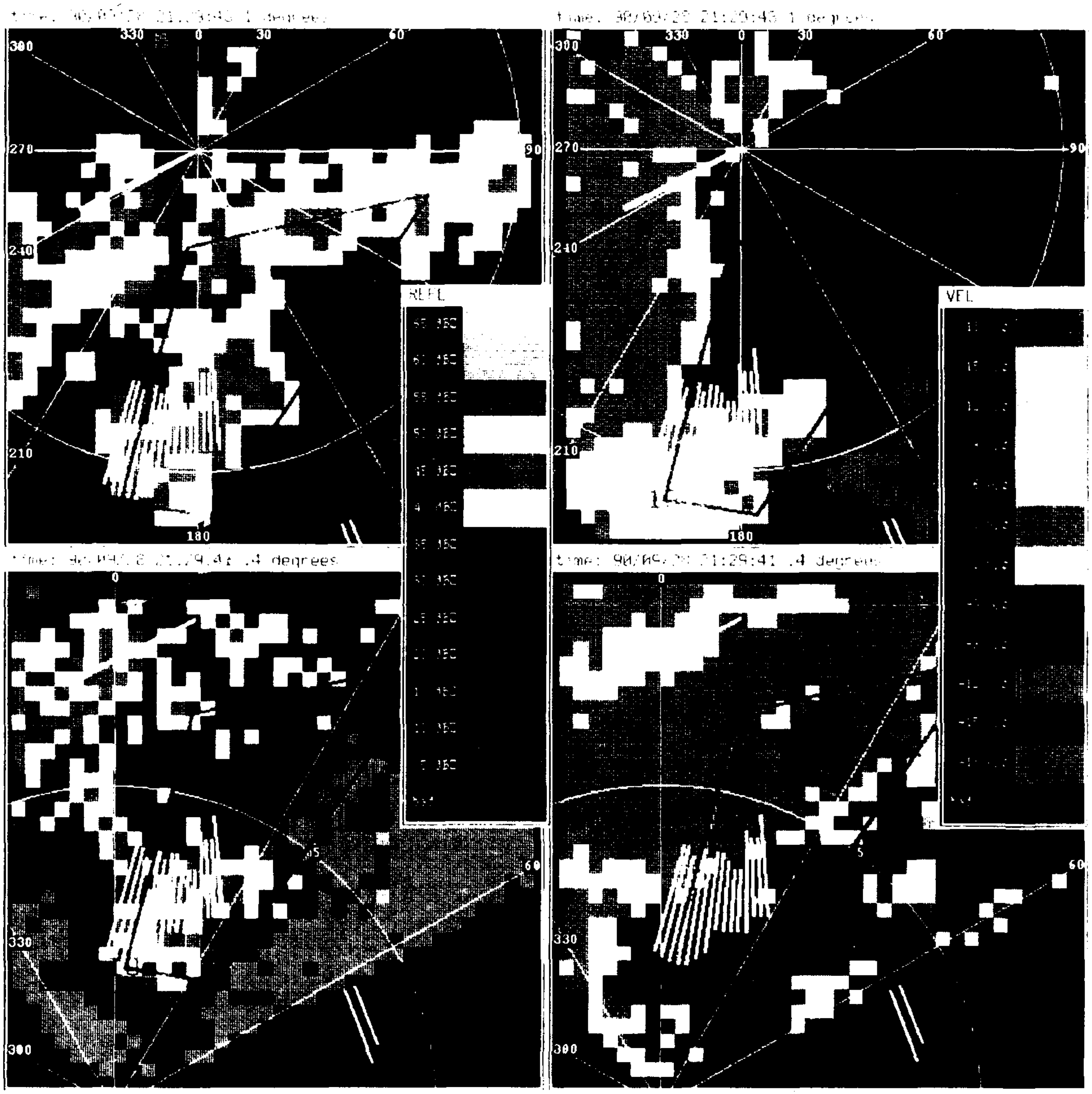

Figure 10. Missed Detection Caused by Algorithm Area Thresholding. Upper left: ASR reflectivity field; Upper right: Divergence segments detected in ASR velocity field near 5 km, 180 degrees; Bottom: Red polygons indicate microbursts observed by FL-2C truth radar

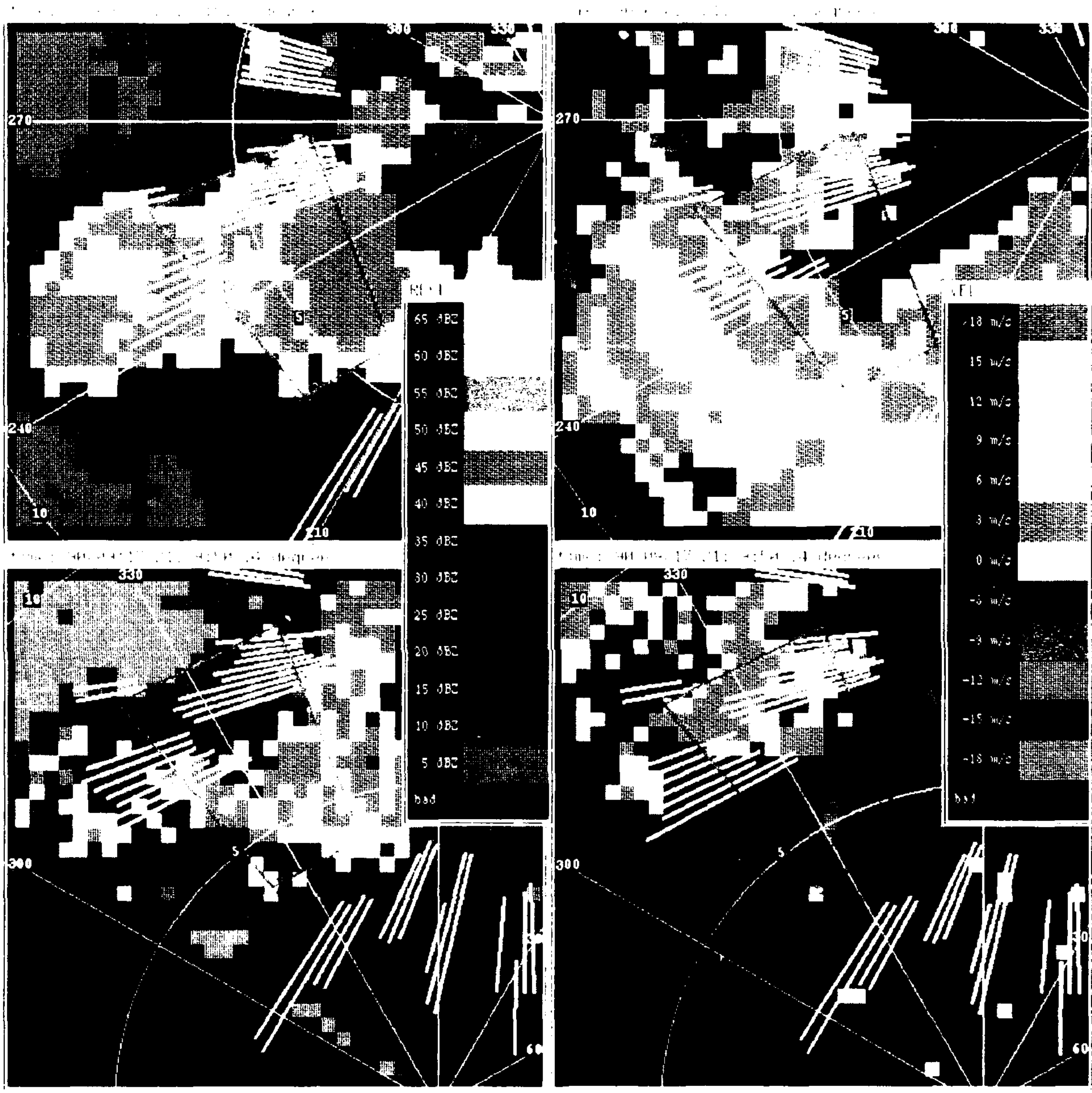

Figure 11. Missed Detection Caused by Algorithm Segment Association Rules. Red polygons indicate microbursts observed by truth radar. Top: Cluster of shear segments found at 7 km, 245 degrees not associated with cluster at 4 km, [illegible] degrees. Bottom: Corresponding data from FL-2C truth radar.

4. GUST FRONT DETECTION

4.1. PRODUCT OVERVIEW

Although the rapid rate of the ASR provides data every 4.8 seconds, computational limitations of the interim gust front algorithm and processing architecture limited the frequency of detection output to once every two minutes. At each two-minute interval, the algorithm received and processed temporally filtered reflectivity and Doppler velocity estimates from a single plan position indicator (PPI) scan. (Reflectivity estimates were smoothed by averaging over the preceding six scans (30 seconds), while velocity estimates were smoothed using a one-pole IIR filter). Gust front locations and forecast positions were updated on the GSD every minute using the most recent detection, if available, or the one-minute forecast in between algorithm updates.

4.2. ALGORITHM DESCRIPTION

Gust fronts can be identified in Doppler pencil-beam weather radar data as a zone of velocity convergence often accompanied by a corresponding reflectivity thin line. Reduced sensitivity owing to an ASR's lower-gain surveillance antenna pattern prevents measurement of velocities associated with clear air echoes ahead and behind the gust front; as a consequence, the convergent velocity signature is not usually apparent in ASR-WSP data. However, SNRs associated with reflectivity thin line echoes are often sufficient to make valid reflectivity and velocity estimates. The current ASR-WSP gust front algorithm relies on reflectivity thin line identification to detect gust fronts. Velocity estimates in the thin line are used to generate estimates of the winds behind the front.

The algorithm can be broken into three stages:

1. Reflectivity thin line feature extraction.
2. Feature association and discrimination.
3. Wind shift and wind shear estimation.

Reflectivity thin line features identified by the feature extraction (FEATX) module are passed, along with statistics derived from associated radial velocity measurements, to the ADM. The ADM utilizes a rule-based approach to associate and discriminate thin line features based on tracking history, spatial proximity, and feature shape and orientation. Gust front detections and gust front forecast positions are the primary data generated by the ADM. Wind velocity statistics for each thin line region are merged with the detection and forecast data for later ingestion and dissemination by the wind shift and wind shear hazard estimation module.

The FEATX module and the ADM are those used in the TDWR Advanced Gust Front Algorithm (AGFA). FEATX and ADM parameters were adjusted to reflect ASR-WSP gust front signature characteristics and are shown in Table 7, page 43. The remainder of this section provides a more detailed description of the algorithm stages. The complete algorithm ran on a single SUN SparcStation.

4.2.1. Thin-Line Feature Extractor - FEATX

The FEATX module utilizes a successive thresholding technique to isolate thin regions of relatively enhanced reflectivity within a radar reflectivity data field. As many as 10 site-adaptable reflectivity thresholds may be specified and are selected to span the anticipated range of gust front thin line reflectivity.

The ASR-WSP reflectivity data are first mapped from their original polar coordinate form onto a 250- x 250-meter resolution cartesian grid. Then, for each threshold level, the module identifies regions with reflectivity above that threshold. Regions which are too small to be part of an actual gust front are removed by thresholding the area of each region against a specified minimum area threshold.

Starting at an arbitrary point on the region boundary, the entire region boundary is traced and transformed into a connected vector representation. The set of outline vectors is then examined to locate pairs of oppositely directed vectors which are within an allowable orientation difference of each other. Such vectors are said to be "anti-parallel." If the anti-parallel vectors are within a specified distance of each other, an intermediate parallel thin-line segment is "drawn" between the two associated anti-parallel vectors on the cartesian grid.

The process is repeated for each reflectivity threshold level, superimposing the intermediate thin-line segments on the grid. Segments from successive reflectivity threshold levels which correspond to gust front thin lines will tend to overlap or occupy proximate grid pixels. A boundary walking algorithm is used to enclose the overlapping and proximate segments, thus forming a bounded thin-line feature representation. Small thin-line features are rejected by imposing minimum area and length thresholds.

Occasionally, downward ducting of the radar beam (anomalous propagation) results in excessive ground clutter breakthrough in which the algorithm may identify reflectivity thin lines. Since these thin lines arise from stationary ground clutter, the associated Doppler velocity estimates are near zero m/s. In order to reduce the likelihood of false alarms due to this phenomena, the module accepts thin-line features only if a sufficient percentage of the associated velocity magnitude estimates exceed a minimum velocity threshold.

4.2.2. Association and Discrimination Module - ADM

The ADM utilizes an extensive rule base, along with spatial and temporal properties to associate and combine valid thin line features into gust front detections and to reject features associated with false alarms. Once the candidate features have been associated and identified as a gust front detection, the module uses tracking history to compute the gust front propagation velocity estimate. This propagation velocity is then used to generate forecasts of future gust front positions at predetermined time intervals. The module can be broken down into three major components: feature scoring, feature merging, and temporal association.

Feature Scoring

The following general rules are used to assign a score to each thin-line feature in order to determine its validity:

1. As feature length and shape eccentricity increase, the score increases;
2. If the average reflectivity across the feature is outside of a specified range expected for gust fronts, the score is lowered; and
3. If the feature is oriented along a radar beam, the score is lowered. This rule discriminates against range-folded echoes which tend to have radial orientation.

Feature Merging

Thin line features are sorted into three categories based on their scores: (1) low-score features, which are discarded immediately; (2) medium-score or "candidate" features, which are subject to further evaluation, and (3) high-score "definite" features, which are retained. The algorithm attempts to merge adjacent candidate features using end-point and orientation-proximity tests in conjunction with guidance from forecasts generated from previous detection histories. The merged features are subsequently fed back into the scoring process. Merged candidate features which meet high-score requirements are promoted and retained as definite features. Although definite features are immediately flagged for retention, an attempt is made to improve their score using the same merging logic.

Temporal Association

After the set of detections for a scan is computed, the ADM attempts to associate each detection with previous detection time histories. This is accomplished by first constructing a vector normal to the local orientation along every point of the current gust front. A score indicating the degree of temporal association is computed based on the number and quality o. time association matches from intersections of the normal vectors with past detections. If the score is sufficiently high, a series of one-minute forecast positions are generated using a block extrapolation technique.

Gust front detections based on ASR-WSP reflectivity thin line features may be intermittent due to feature fragmentation caused by insufficient radar sensitivity or clutter breakthrough. The ADM provides the capability to "coast" gust front detections (using previously generated forecast positions) for a specified number of scans or until it is able to associate a new detection with the prior detection time history.

Because thin-line fragmentation and detection intermittence tend to increase with decreasing range from the radar due to ground clutter interference, a longer coast period is required to cover the interval during which the gust front is passing over the radar. The ADM permits specification of two independent coasting durations which are applied over two specified range intervals. The current ASR-WSP implementation permits a gust front

detection to be coasted for eight scans (16 minutes) for detections occurring inside 10 km and for three scans (six minutes) for prior detections occurring between 10 and 30 km. In either case, at least three previous detections with an associated propagation velocity of at least 2.5 m/s are required before coasting will be activated. Coasted detections are automatically added to the associated gust front detection time history. Wind shear hazard estimates are coasted along with their corresponding detections.

Finally, to guard against issuing spurious singular detections, a detection is required to have been seen on at least one previous scan before the current detection data is output by the algorithm.

4.2.3. Wind Shift and Wind Shear Hazard Estimation

Estimates of the expected wind speed and direction behind the gust front (wind shift) as well as the wind shear across the gust front are generated for each gust front detection issued by the ADM. The calculation of these quantities is shared between the FEATX module and the ADM.

Given radar sensitivity sufficient for measurement of winds ahead of and behind the gust front, the wind shift and wind shear estimates should be calculated from radial velocity data gathered within representative regions ahead of and behind the front. Since the region between the gust front boundary and the generating storm cell, as well as the region ahead of the front, is usually precipitation free, the ASR often does not reliably measure Doppler velocities within these regions. Therefore, the only available velocity estimates associated with the gust front are those corresponding to the reflectivity thin line. The FEATX module uses these thin line velocity estimates to compute the mean radial wind speed for each thin line feature. This mean radial wind speed is used in conjunction with the gust front propagation direction calculated by the ADM to derive the wind shift and wind shear hazard estimates.

The wind shift product consists of two quantities: the wind speed behind the front, and the wind direction behind the front. The wind speed behind the front is calculated in the FEATX module by averaging the magnitudes of the radial velocity estimates within the reflectivity thin line region. This approach assumes that the thin line velocity estimates are representative of the expected wind speed change after passage of the gust front. The wind direction behind the front is taken to be the gust front propagation direction computed in the ADM.

The wind shear estimate represents the change in wind speed (ΔV) across the gust front. Since the majority of summertime thunderstorms in Orlando develop in air which is relatively calm, the wind shear was calculated by first assuming that the environmental wind speed ahead of the gust front is zero. With this assumption, the ΔV across the front is simply equal to the wind speed immediately behind the frontal boundary.

Table 7. ASR-WSP Gust Front Algorithm Parameters

PARAMETER NAME	DESCRIPTION	SETTING
THRESH_[X], X = 1,2,3,4,5	Reflectivity threshold levels for thin line feature extraction.	3.5, 5.0, 7.5, 9.0, 12.0 dBZ
MAX_SEG_ANGLE	Maximum allowable "anti-parallel" segment pair orientation difference during thresholding phase.	0.40 rad
MAX_SEG_DIST	Maximum allowable "anti-parallel" segment distance during thresholding phase.	4.0 km
MIN_REGION_AREA	Minimum area required for regions generated by the thresholding phase.	4.0 km^2
MIN_FEAT_AREA	Minimum required thin line feature area.	4.0 km^2
MIN_FEAT_LEN	Minimum required thin line feature length	7.0 km
MAX_FEAT_RANGE	Distance beyond which features are rejected because of possible data edge effects.	25.0 km
MIN_VEL_THRESH	Minimum required velocity within a thin line feature.	2.0 m/s
PCT_GOOD_VEL	Minimum required percentage of velocity estimates above MIN_VEL_THRESH for a thin line feature.	75.0 %
LOW_DBZ_THRESH	Minimum required average thin line reflectivity	0.0 dBZ
HIGH_DBZ_THRESH	Maximum required average thin line reflectivity	20.0 dBZ
PARALLEL_THRESH	Minimum thin line feature orientation angle relative to radar beam azimuth.	8.0 deg
COAST_MIN_DETECTS	Minimum number of prior detections required before activating coasting.	3
COAST_MIN_VEL	Minimum required gust front propagation velocity for coasting.	2.5 m/s
MAX_COAST_1	Maximum allowable number of coasts in 1st range interval.	8 scans
COAST_RANGE_1	Range interval over which MAX_COAST_1 applies.	0 - 10 km
MAX_COAST_2	Maximum allowable number of coasts in 2nd range interval.	3 scans
COAST_RANGE_2	Range interval over which MAX_COAST_2 applies.	10 - 25 km

4.3. ALGORITHM PERFORMANCE

4.3.1. Performance During the ASR-WSP Operational Demonstration

Comments noted by TRACON and Tower observers indicate an overall satisfaction with the ASR-WSP gust front detection capability. Supervisors found the product to be a valuable aid in coordinating air and ground traffic in anticipation of airport runway reconfigurations. In spite of the limited number of thunderstorm days during the operational period, the algorithm successfully identified 15 gust fronts.

Algorithm parameter and code modifications were necessary during the operational period to alleviate unanticipated false declaration problems. As a result, algorithm perform-

ance improved during the course of the demonstration period. Although there were roughly 25 false declarations, none of these impacted the airport runway or caused an alert to be issued. False declarations generally occurred in the presence of three different types of weather reflectivity phenomena which are listed here in decreasing order of prevalence:

1. Range-folded (second-trip) echoes.
2. Small, isolated clouds or precipitation regions.
3. Enhanced clutter breakthrough during anomalous propagation (AP).

Nearly all of the false declarations occurred in conjunction with the first two listed phenomena. False declarations arising during AP episodes were practically eliminated by imposing a non-zero radial velocity requirement for thin-line reflectivity regions (see Section 4.2.1.).

As discussed in Section 1.2.1, the algorithm attempts to discriminate against radially-oriented reflectivity features associated with range folding by comparing the orientation angle of the feature against the radar beam azimuth angle which passes through the feature centroid. A least squares regression is used to calculate the line which represents the feature orientation. False declarations tended to occur whenever range-folded echoes were curved or hooked, causing the calculated feature orientation angle to deviate significantly away from the radar azimuth angle. Although using a larger angle threshold may have rejected some of the false declarations, this would also increase the risk of rejecting valid thin-line features. Requiring at least two successive algorithm declarations before dissemination proved successful in reducing the number of spurious singular false declarations arising from this phenomenon. Alternate methods for discrimination of range-folded echoes are currently being examined.

False declarations also occurred when the algorithm mistook small, isolated clouds and precipitation regions to be thin lines. This problem was most evident during a stratiform rain period on September 29. On that day, the algorithm issued a number of false declarations in connection with embedded heavy-intensity rain bands within the widespread light precipitation. Since gust fronts occur in connection with high-reflectivity thunderstorms, imposing a criterion requiring a high-reflectivity region or gradient in the vicinity of a gust front may reduce the number of false declarations during these weak stratiform precipitation periods.

4.3.2. Selected Case Study Analysis

Gust fronts observed by FL-2C and identified by a meteorologist were used as the source of truth for comparison against algorithm output. Only those gust fronts which tracked over the airport and were identified as having moderate (10 m/s $\leq \Delta V <$ 15 m/s) to strong (15 m/s $\leq \Delta V <$ 20 m/s) wind shear were used for this preliminary case study analysis. Unfortunately, an abnormally low incidence of thunderstorms during the ASR-WSP demonstration period resulted in only three gust fronts which impacted the airport, and only one (September 17) that was strong enough to qualify for this assessment. Therefore, an additional six gust front events which occurred prior to the demonstration period

were evaluated by running the ASR-WSP gust front algorithm on previously recorded data obtained during combined TDWR testbed (FL-2C) and ASR-WSP operations. Although multiple gust fronts were present during some of the periods, only one gust front during each scoring period met the above mentioned wind shear strength criteria.

Table 8 summarizes the events scored. The table lists the maximum differential velocity across the gust front observed by FL-2C during the event as well as an indication of whether the associated wind shear was sufficiently strong (ΔV > 15 kts) during airport impact that a wind shear alarm should have been generated.

Table 8. Summary of FL-2C Gust Front Events Used for Scoring

DATE	TIME PERIOD SCORED (UT)	MAXIMUM OBSERVED DIFFERENTIAL VELOCITY (m/s)	AIRPORT ALARM?
July 12	2208 - 2220	22.0	Yes
July 13	1915 - 1933	22.0	Yes
July 25	2041 - 2156	14.0	Yes
August 10	2252 - 2356	18.0	Yes
August 11	1900 - 1924	14.0	Yes
August 14	1753 - 1825	10.0	No
September 17	2011 - 2017	10.0	Yes

4.3.3. Scoring Method

For the preliminary assessment, a hit-miss criterion was used for scoring the gust front algorithm. A more detailed assessment will follow in a future report. For each of the selected gust front events, algorithm output was examined and scored by comparison with FL-2C data to determine:

1. What percentage of moderate to strong gust fronts were detected by the algorithm?
2. What percentage of gust fronts that crossed the airport were detected prior to their arrival?
3. What percentage of gust fronts generated runway alarms where appropriate?
4. How accurate were the wind shear hazard estimates?

4.3.4. Scoring Results

The following is a summary and description of the algorithm scoring results. Algorithm performance is summarized in Table 9, page 47.

Overall Detectability

Four out of seven gust fronts were successfully detected during the course of the event. There were no false declarations during the selected periods; however, the limited data sample precludes meaningful computation and extrapolation of false declaration probabilities.

Three of the seven gust front events examined went undetected by the ASR-WSP gust front algorithm. Two of the missed events were in the moderate shear strength category, and one was in the strong shear strength category. In all three of the missed events, thin line features were only marginally evident in the ASR base data, or they were absent altogether. Thin-line features were visible in FL-2C base data during all three missed events.

Advance Warning

A detection prior to airport arrival was generated for only one of the six gust fronts examined (the gust front of August 11 is excluded here because of lack of available data from the ASR prior to airport-impact). The gust front of September 17 (the only moderate-strength gust front during the operational test) was detected 25 minutes in advance of airport impact. This gust front generated a thin line that was distinct and already well-separated from the generating storm cell as it came within range of the radar.

Of the remaining five gust fronts, four had not yet propagated ahead of the generating storm and did not appear as distinct thin lines until after airport passage. Thus, the gust front algorithm did not provide advanced warning for these four cases. However, some degree of warning would have been provided by the storm motion algorithm since in these cases, the gust fronts were closely associated with the leading edge of advancing storms containing heavy precipitation. Also, a pre-frontal environmental wind measurement (e.g., from LLWAS) could be used in conjunction with the ASR-WSP velocity measurements in the precipitation behind the front to infer the convergence associated with the gust front at the leading edge of the storm.

The fifth gust front (August 10) had an associated thin line which rapidly became fragmented as it approached and passed over the radar.

Airport Alarms

As reported by FL-2C, six of the seven gust front events were of sufficient shear strength to have produced an alarm upon airport impact. The ASR-WSP algorithm generated a wind shear alert for two of these six events. All four misses were due to the same absence of thin line signatures, which caused the advance warning failures mentioned above.

Accuracy of Wind Shear Hazard Estimates

Comparison of Tables 8 and 9 indicates that for the four detected events, the maximum ΔV estimated by the algorithm was smaller--sometimes significantly smaller--than the maximum ΔV observed by FL-2C. This suggests that opposing environmental wind compo-

nents were present for each of these gust fronts, and that the assumption of near-zero environmental wind speed by the gust front algorithm was inappropriate for estimation of the associated wind shear hazard.

Table 9. Preliminary ASR-WSP Gust Front Algorithm Results for Orlando, FL

DATE	ALGORITHM DETECTION	ADVANCED WARNING?	MAXIMUM DIFFERENTIAL VELOCITY (m/s)	AIRPORT ALARM?
July 12	Yes	No	11.0	No
July 13	Yes	No	10.0	No
July 25	No	No	--	No
August 10	No	No	--	No
August 11	Yes	No*	10.0	Yes
August 14	No	No	--	No
September 17	Yes	Yes	8.0	Yes

* Lack of available data prior to airport impact prevented earlier detection.

4.4. FUTURE WORK

The following work is ongoing and should result in significant improvements in algorithm performance:

1. Case study analysis to identify current algorithm weaknesses and failures.
2. Further optimization of current algorithm parameters.
3. Development of an improved thin-line detection algorithm.
4. Additional testing and development of algorithms for discrimination of false detections arising from AP-induced ground clutter and range-folded echoes.
5. Development of algorithms which make appropriate use of ASR-WSP velocity data (possibly in conjunction with LLWAS data) to derive accurate wind shear and wind shift estimates.
6. Improvement of reflectivity and velocity estimates for low SNR weather. This will be accomplished through a combination of front-end radar modifications and signal processing algorithm enhancements.

5. STORM MOTION

5.1. PRODUCT OVERVIEW

The storm motion algorithm (SMA) was developed for the TDWR as an aid to air traffic planning in the terminal area. The SMA tracks the movement of significant storm cells using a correlation-based cell-tracking algorithm. [6] The techniques employed for tracking storm movement in the TDWR domain are equally applicable to the precipitation reflectivity data generated by the ASR-WSP and were easily incorporated into the ASR-WSP operational system.

The storm motion vectors were updated every three minutes on the GSD for the ASR-WSP demonstration.

5.2. ALGORITHM DESCRIPTION

The SMA can be broken down into three stages: (1) primitive motion detection; (2) storm feature identification, and (3) integration of the output of (1) and (2) to provide storm motion estimates. The techniques employed in these three stages are summarized below.

5.2.1. Primitive Motion Detection

The six-level precipitation map is input to the SMA. The first stage of the SMA computes image motion independent of any higher-level information. A cross-correlation technique is used to measure image displacement between time frames by calculating a cross correlation matrix. The cross-correlation function is produced by the following steps:

1. Thresholding the precipitation map at a user-specified level to produce a binary image;
2. Partitioning the binary image into smaller "correlation boxes;" and
3. Tracking each binary sub-image from one time frame to the next.

This process yields a field of displacement vectors. The vectors are subjected to spatial median filtering and temporal smoothing before being input to the integration process.

5.2.2. Storm Feature Identification

A storm is defined as a connected set of resolution cells falling between two reflectivity values (corresponding to a NWS reflectivity level.) To identify significant storm features, storms at a maximum level (MAX_LEVEL) are isolated and subjected to a minimum size criterion, and their centroids are computed. The next NWS level down is processed, and centroids are computed for all storms that do not underlie an existing storm (at the level above). This process is repeated for the remaining levels, down to a user-specified minimum level (MIN_LEVEL).

Centroid locations are sorted by the corresponding storm level and storm size. The most significant (MAX_OUTPUTS) centroids are retained.

5.2.3. Integration

The integration step produces storm movement predictions by associating the spatially and temporally smoothed track vectors with the storm features.

Table 10 lists operationally significant SMA parameters used for the 1990 operational testing.

Table 10. Storm Motion Algorithm Parameters

PARAMETER NAME	DESCRIPTION	SETTING
UPDATE_TIME	Amount of time between product updates.	3 minutes
MIN_LEVEL	Minimum detected NWS level for storm core.	3
MAX_LEVEL	Maximum detected NWS level for storm core.	6
MIN_STORM_SIZE	Minimum size for detected storm.	5 km^2
MAX_OUTPUTS	Maximum number of vectors to be displayed.	5

6. AIR TRAFFIC OPERATIONAL ASSESSMENT

Following the ASR–WSP demonstration the FAA Technical Center distributed a questionnaire to Orlando Air Traffic Control personnel to obtain their assessment of system performance. Forty–nine persons responded to the survey, but many did not answer all the questions. Results of the questions have been tabulated below in histogram form. Respondents were invited to elaborate on questions with written comments; the comments have been included.

6.1. AIR TRAFFIC CONTROL QUESTIONNAIRE RESULTS

Question 1: Please rate different aspects of the ASR–WSP using the following scale:

+3 = Very good
+2 = Good
+1 = Fairly good
0 = Fair
–1 = Fairly poor
–2 = Poor
–3 = Very poor
? = Don't know

A. Daytime readability of the display

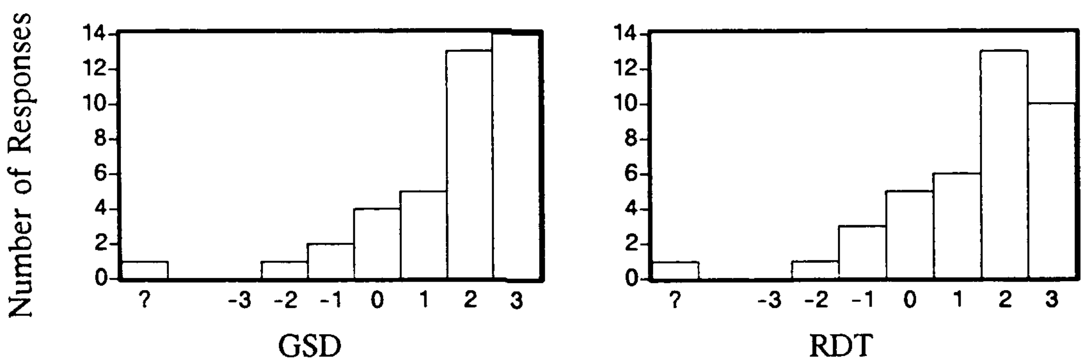

B. Nighttime readability of the display

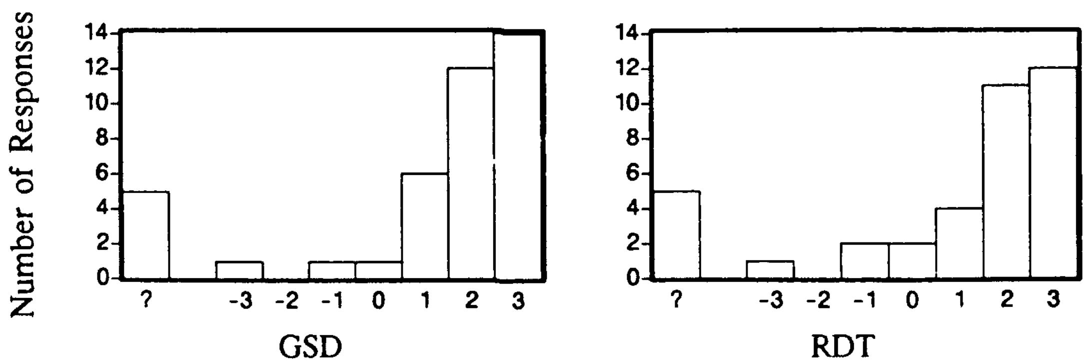

C. Readability of display in glare

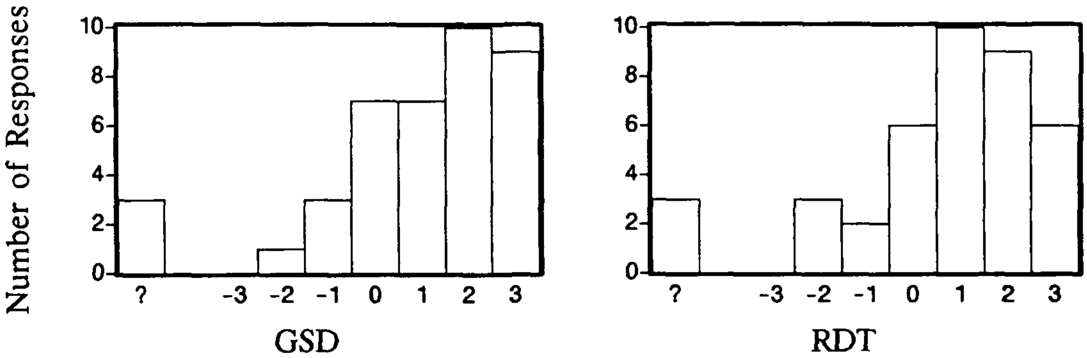

D. Noticeability of blinking messages

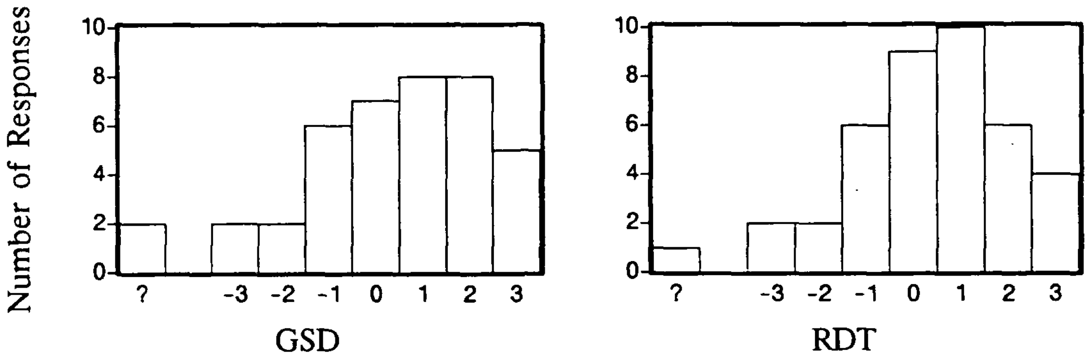

E. Audibility of the alarm beeper

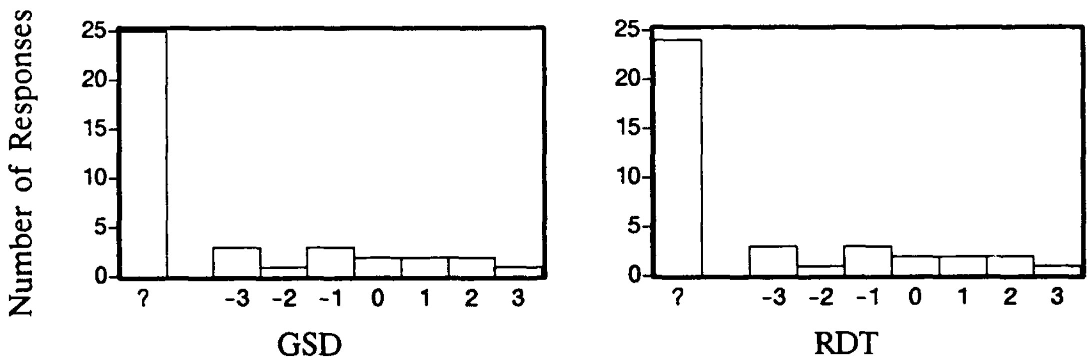

F. Placement of the display

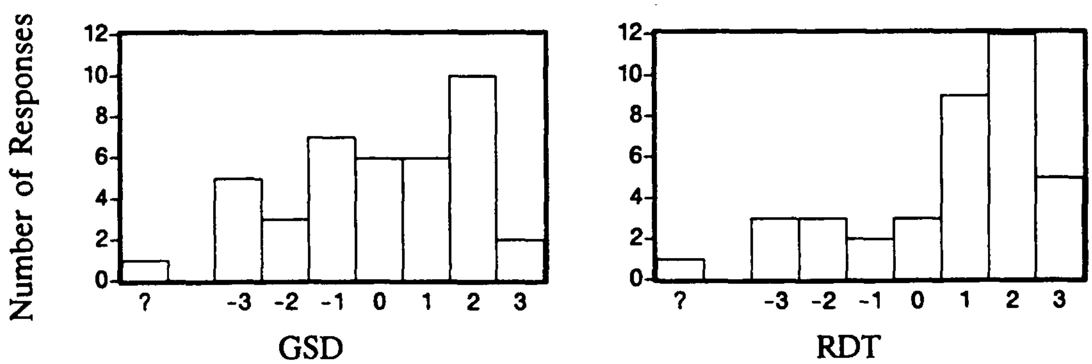

G. Completeness of the displayed information

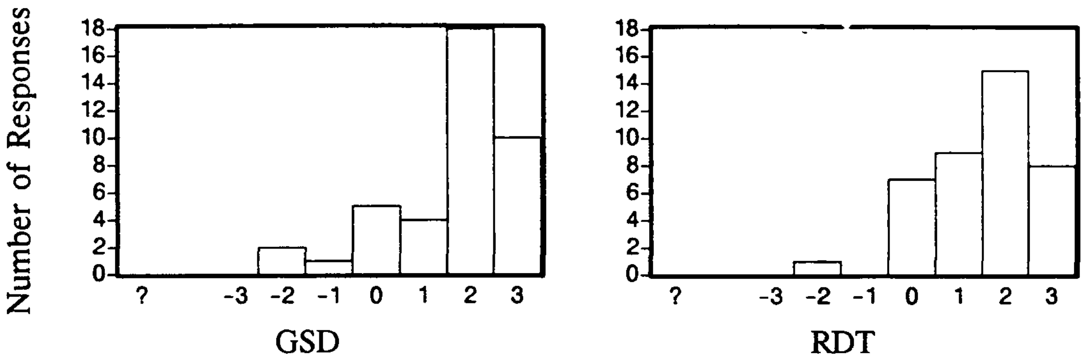

H. Accuracy of the displayed information

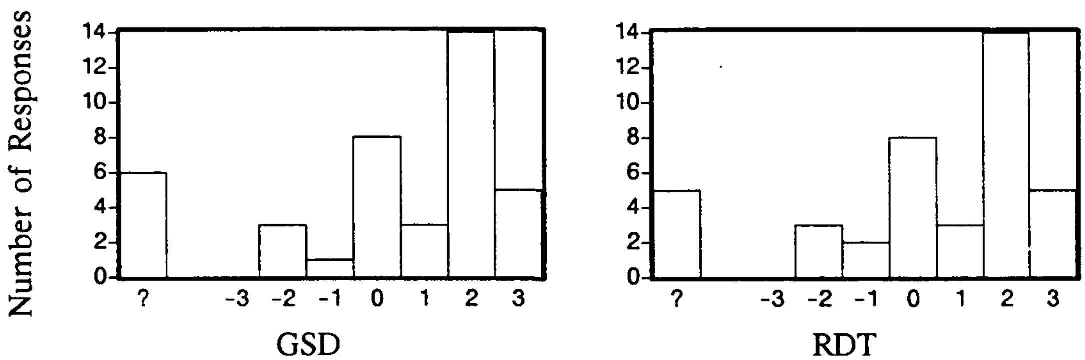

I. Rate of false alarms (many = −3, few = +3)

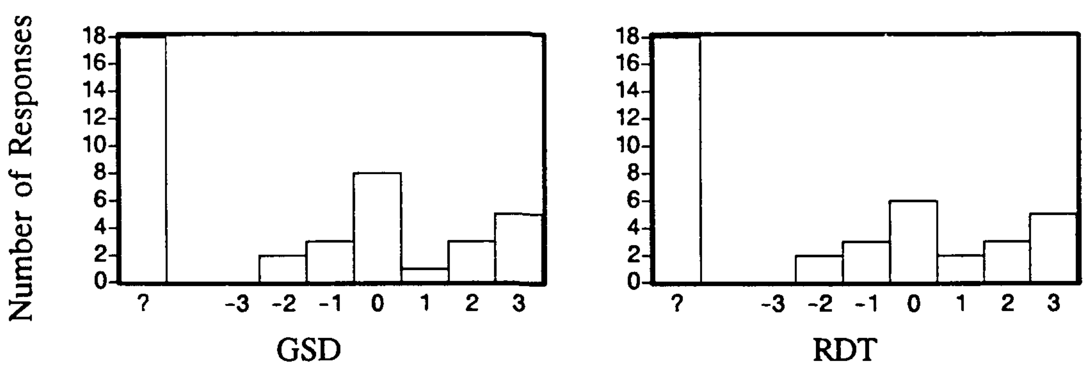

J. Timeliness of the displayed information

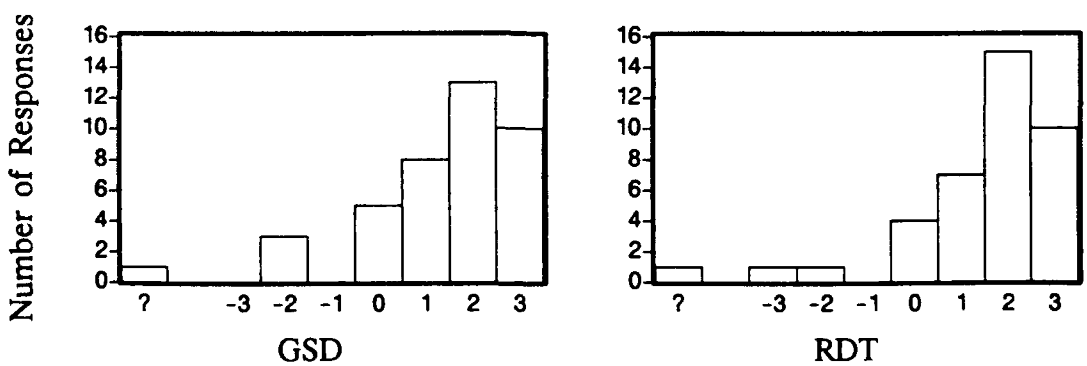

K. Usefulness of the displayed information

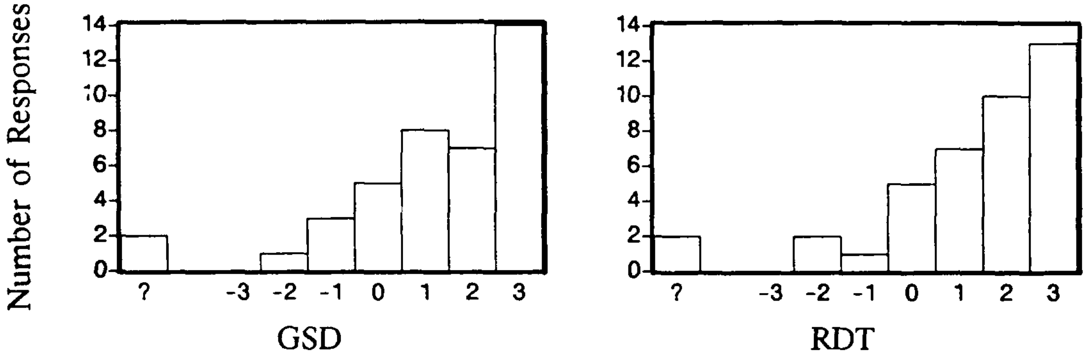

L. Freedom from misinterpretation

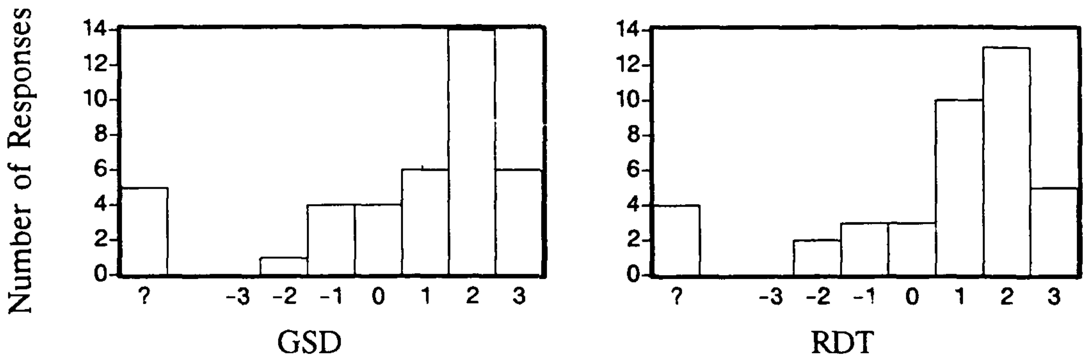

M. Ease of accessing needed wind information

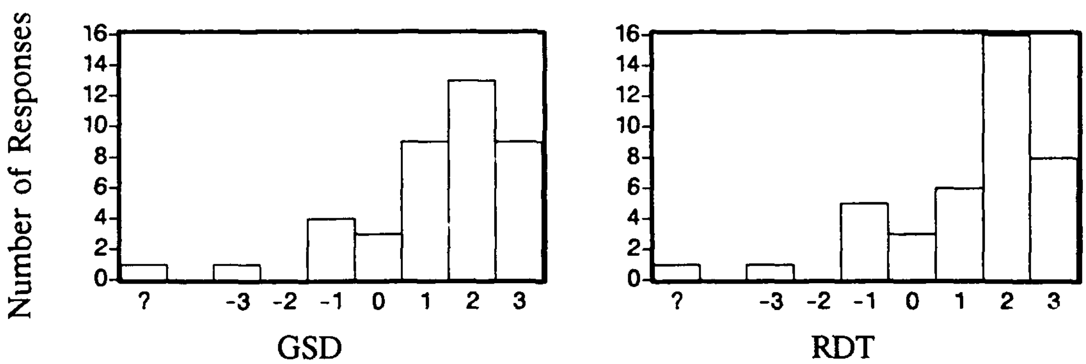

N. Speed of system response

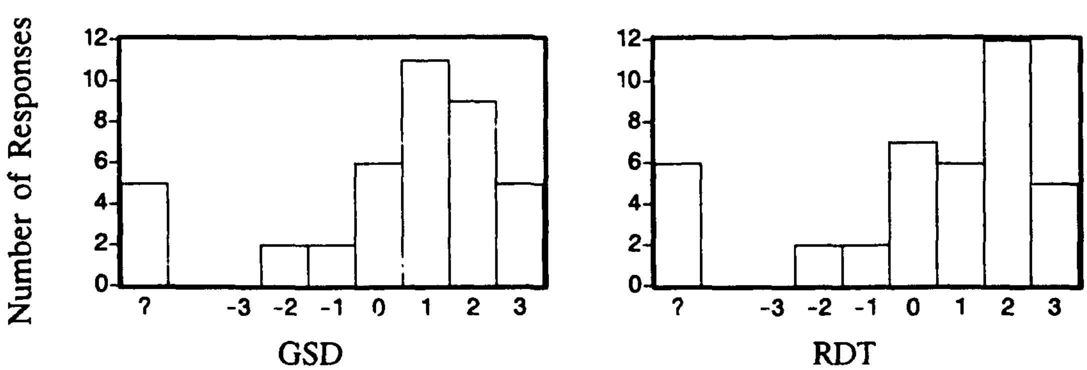

O. Information grouping and order within rows

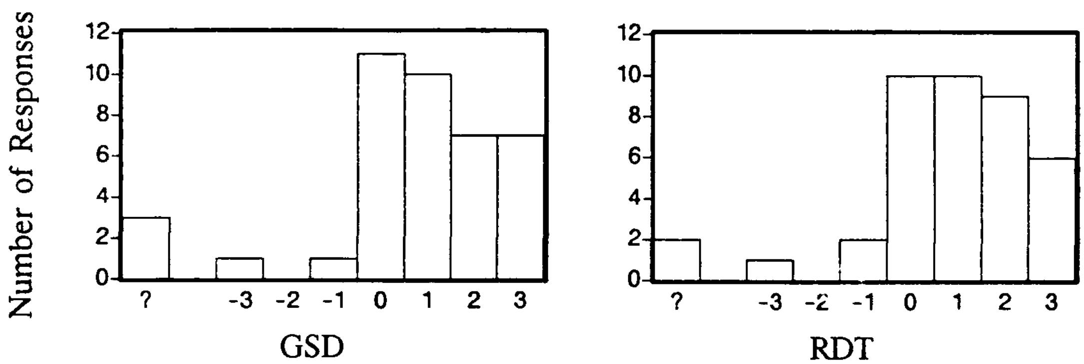

P. Aptness of message abbreviations

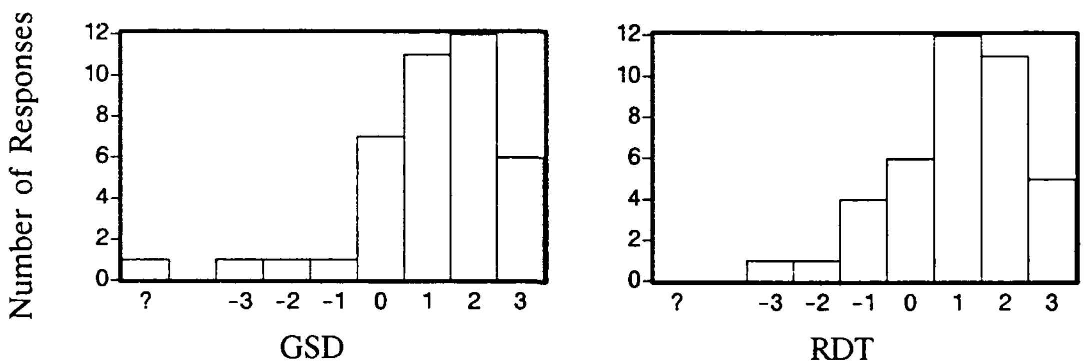

Q. Naturalness of spoken phraseology

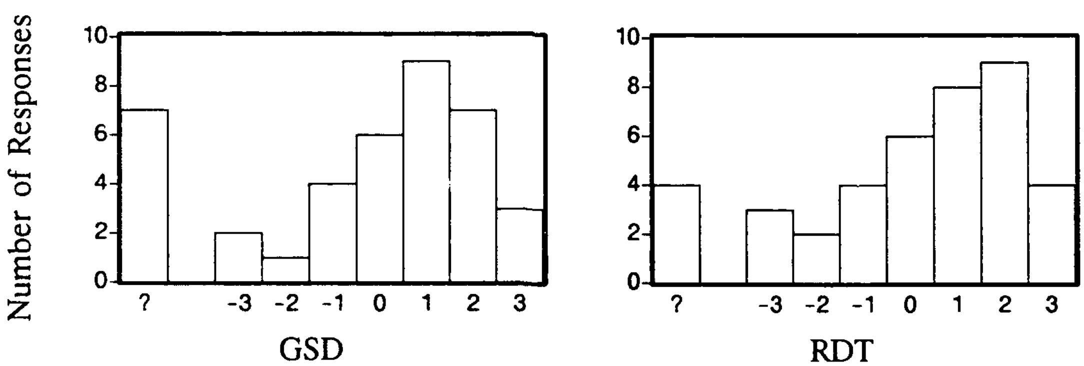

R. Suitability for continued field use

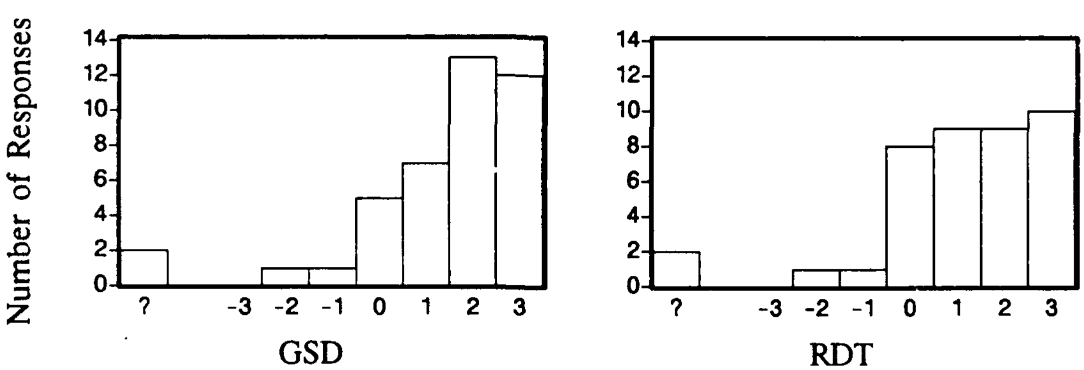

S. Usefulness of wind arrows on GSD

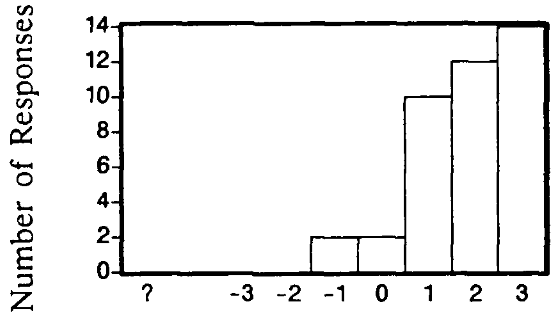

T. Usefulness of gust front presentation

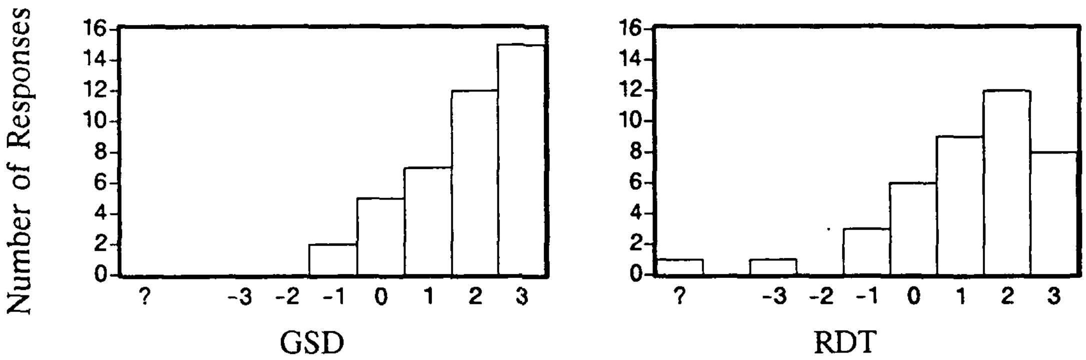

U. Usefulness of the wind shift prediction

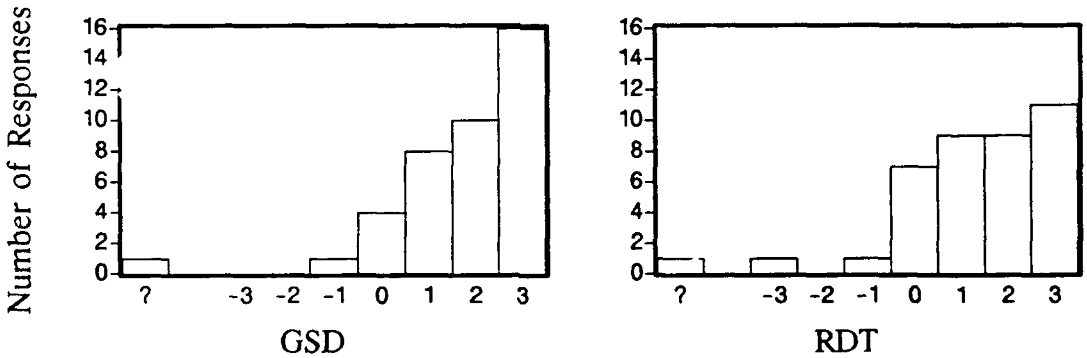

V. Usefulness of the ASR-WSP training received

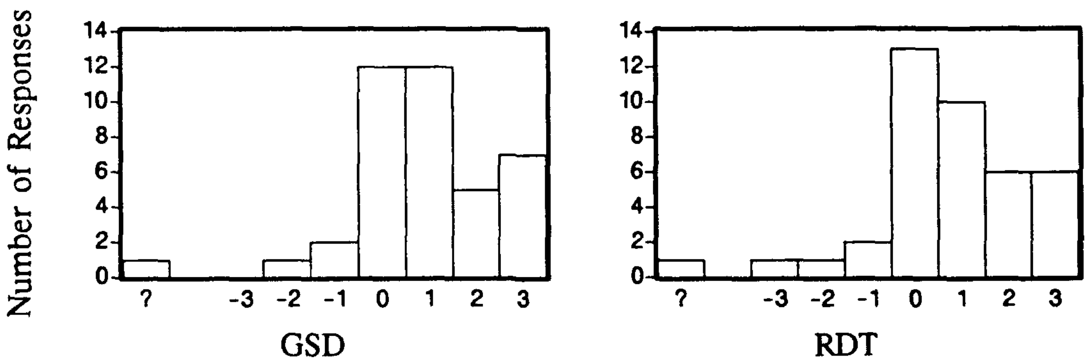

W. Usefulness of the ASR–WSP runway management

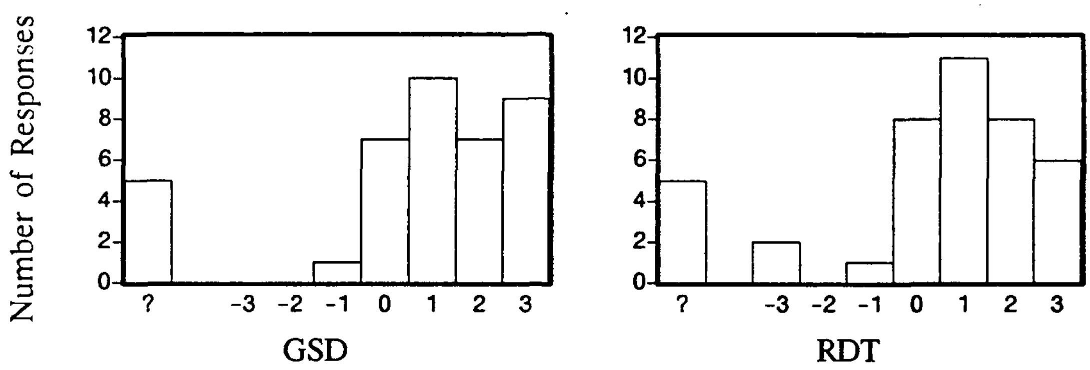

User Comments in Response to Question 1

- "During up time there was not enough weather present to evaluate the system."
- "Traffic was stopped on the basis of the presentation -- if it had not been operational aircraft would have departed and landed without incident."
- On the RDT:
  "Monitors for RDT were too large and obstructed visibility."
- On the GSD:
  "Need a GSD for each position in the Tower and at least 5 or 6 in the TRACON."
- On the ARTS display:
  "Excellent tool for radar controllers."

  "The presentation was not clear and distinct enough to be useful. It appeared fuzzy and washed out on the display."

  "It would be hard to get a good presentation without interfering with display of aircraft targets and map."

Use the following scale to answer questions 2 through 4:

+3 = A great help
+2 = A help
+1 = A slight help
0 = Neither help nor hindrance
–1 = A slight hindrance
–2 = A hindrance
–3 = A great hindrance
? = Don't know

Question 2: Do you see the ASR-WSP as a help or a hindrance to you in your job of controlling local traffic?

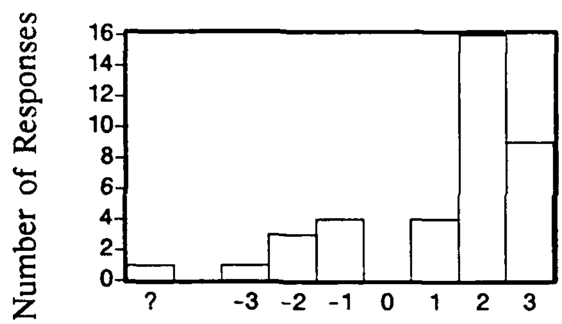

User Comments in Response to Question 2

- "Cuts down traffic to a standstill."
- "False alarms need to be minimal."
- "It it can prevent people getting killed, so what if a few aircraft get delayed."
- "Too much attention needed for accurate timely use."
- "This information should be given in the cockpit directly to the crew."

Question 3: Do you see the ASR-WSP as a help or a hindrance to the pilot?

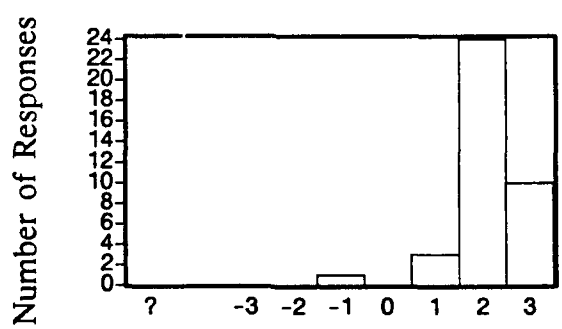

User Comments in Response to Question 3

- "If false alarms are minimal, ASR-WSP can be a great help."
- "Airline company procedures require pilots to hold on the ground or go around when a microburst alert is issued. More education is required to change this procedure. Example: a microburst on 3 miles final should not have impact to a departing airplane, but procedures will not permit a departure."

Question 4: Do you see the ASR-WSP as a help or a hindrance to the planning and training management?

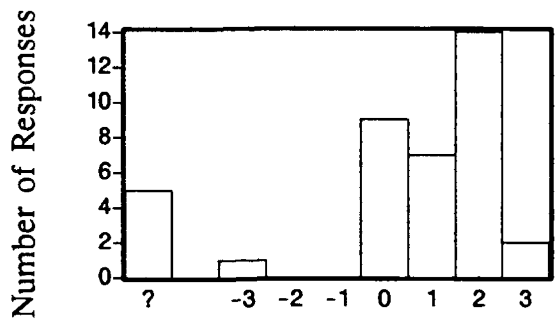

Question 5: What is good about the ASR-WSP? What benefits do you see?

User Comments in Response to Question 5

- "Wind shift prediction for optimum runway utilization."
- "Preplanning traffic flows."
- "Display of weather areas in levels."
- "Timely information."
- "Helps tie down the position of the actual wind shear."

Question 6: What is poor about the ASR-WSP? What problems do you see?

User Comments in Response to Question 6

- "Until perfected there are no benefits."
- "Use of word microburst became a scare tactic."
- "Too much burden placed on controllers to ensure pilot gets current wind shear information -- this should not be an ATC function."
- "Too many false alarms."
- "It does not update often enough."

Question 7: Please rate the relative magnitude of the benefits and problems of the ASR–WSP.

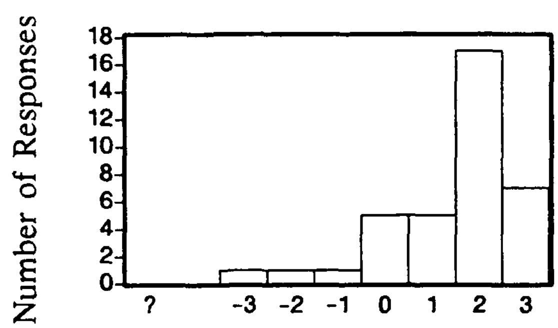

Question 8: Compare the overall effectiveness of the prototype ASR–WSP to the LLWAS.

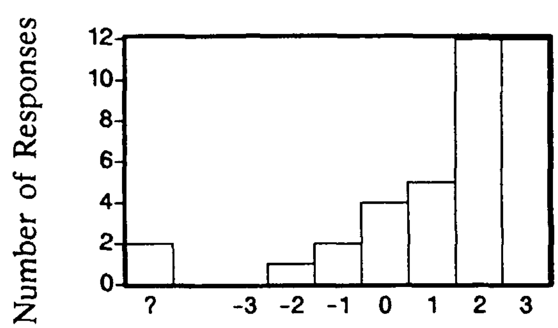

Question 9: Based on your present knowledge, please rate the ASR–WSP's suitability for widespread operational use in the field.

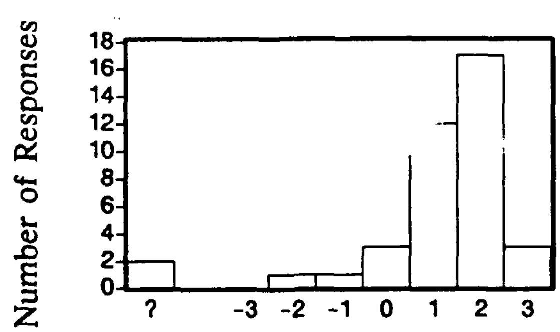

Question 10: Based on your present knowledge, please rate the ASR-WSP's usefulness to the pilot.

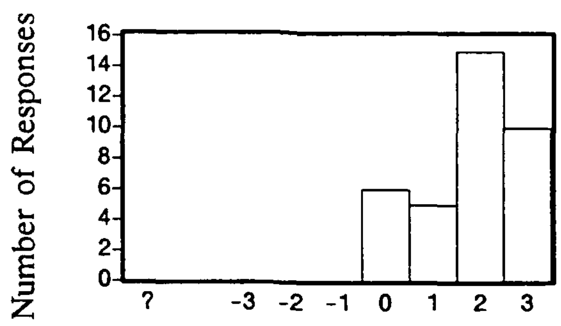

User Comments in Response to Question 10

- "Make this information available to the pilots and leave ATC out. Rapidly changing information cannot be the responsibility of the Tower controller. ATC has too much to do now -- one missed microburst could be life threatening and this burden should not be placed on our shoulders."

REFERENCES

1. D.M. Bernella (ed.), "Terminal Doppler Weather Radar Operational Test and Evaluation Orlando 1990," *Project Report ATC-179*, Lincoln Laboratory, DOT/FAA/NR-91/2, (1991).

2. M.E. Weber, T.A. Noyes, "Wind Shear Detection with Airport Surveillance Radars," *Lincoln Laboratory Journal*, **2**, 511 (1989).

3. M.E. Weber, "Dual-Beam Autocorrelation Based Wind Estimates from Airport Surveillance Radar Signals," *Project Report ATC-167*, Lincoln Laboratory (1989), FAA-PS-89-5.

4. M.M. Wolfson, "Characteristics of Microbursts in the Continental United States," *Lincoln Laboratory Journal*, **1**, 49 (1988).

5. D.L. Klingle, D.R. Smith, M.M. Wolfson, "Gust Front Characteristics as Detected by Doppler Radar," *Monthly Weather Review*, the American Meteorological Society, **115**, 5 (1987).

6. E.S. Chornoboy, Personal Communication, Lincoln Laboratory, MIT, September 1990.

7. C. Biter, *TDWR/LLWSAS User Working Group, Summary of the 15–17 February 1989 Meeting*, National Center for Atmospheric Research, Boulder, CO (1989).

8. S.D. Campbell, P.M. Daly, R.J. DeMillo, "An Experimental Cockpit Display for TDWR Wind Shear Alerts," *Proc. 4th International Conference on Aviation Weather Systems*, Paris, France, June 1991.

9. M.W. Merritt, "Automated Detection of Microburst Wind Shear for Terminal Doppler Weather Radar," *Proc. Digital Image Processing and Visual Communications Technologies in Meteorology, SPIE* **846**, 61 (1987).